Sunspot Simulations @ The Different Spatio-temporal Scales of Solar Magnetism

Mark Cheung, cheung@lmsal.com (with material from Matthias Rempel)
Lockheed Martin Solar & Astrophysics Laboratory

Overaching questions about sunspots

- Why are sunspots dark? 😎
- Measurement of intense magnetic fields by Hale (1908)
- Intense magnetic fields inhibit convection, thereby reducing convective heat transport (Bierman 1941).
- What are sunspots so bright though? 🥺
- Why does inhibition of convection not channel heat flux around the sunspot, leading to a bright ring?
- Spruit (1978) argued that for deeply anchored (d > 10 Mm) sunspots, efficient convection (close to adiabatic gradient) will wash out the bright ring.
- Parker (1955, and later papers) argue that horizontal pressure balance between 3 kG umbral field and ambient CZ requires lower internal temperatures, thus lower vertical pressure support. Parker argues the intense magnetic field is a consequence of reduced temperature.

Parker (1974)

THE NATURE OF THE SUNSPOT PHENOMENON

I: *Solutions of the Heat Transport Equation* *

2. An Alternative View

The purpose of this paper is to point out that the inhibition of convection seems of secondary importance in the formation of sunspots, if it plays any role at all. Not only does it predict a bright ring around sunspots, but it enhances the subsurface temperatures, which would disperse the magnetic field. We simply cannot account for a sunspot by blocking off the heat flow from below.

Instead we assert that the sunspot occurs as the immediate consequence of the *vigorous* energy transport in the strong magnetic field. The magnetic field causes a major portion of the heat flux to be converted to Alfvén waves, to which the entire Sun is *transparent*. The dynamical overstability is the heat engine that makes the conversion. The result of the transparency is rapid cooling of the conversion volume beneath the sunspot. So heat transport is not blocked by the magnetic field. It is enhanced. Then if there is any ring around the umbra, the ring is dark, because the umbra is effectively a refrigerator. Presumably the penumbra is the dark ring, although other effects probably contribute to the penumbra too (Danielson, 1961a, b).

Parker (1974)

THE NATURE OF THE SUNSPOT PHENOMENON

I: *Solutions of the Heat Transport Equation**

2. An Alternative View

The purpose of this paper is to point out that the inhibition of convection seems of secondary importance in the formation of sunspots, if it plays any role at all. Not only does it predict a bright ring around sunspots, but it enhances the subsurface temperatures, which would disperse the magnetic field. We simply cannot account for a sunspot by blocking off the heat flow from below.

Instead we assert that the sunspot occurs as the immediate consequence of the *vigorous* energy transport in the strong magnetic field. The magnetic field causes a major portion of the heat flux to be converted to Alfvén waves, to which the entire Sun is *transparent*. The dynamical overstability is the heat engine that makes the conversion. The result of the transparency is rapid cooling of the conversion volume beneath the sunspot. So heat transport is not blocked by the magnetic field. It is enhanced. Then if there is any ring around the umbra, the ring is dark, because the umbra is effectively a refrigerator. Presumably the penumbra is the dark ring, although other effects probably contribute to the penumbra too (Danielson, 1961a, b).

What about sunspots could/should models capture?

This movie shows Stokes V images (proxy of line-of-sight field) in a Zeeman sensitive-line of a sunspot.

Salient observational facts:

- Penumbral filaments
- Weaker field in the penumbra than in the umbra
- Moving magnetic features stemming from the penumbra
- Evershed flow
- Possible existence of light bridges
- The sunspot maintains coherence over at least 1 day, though it is continuously evolving.

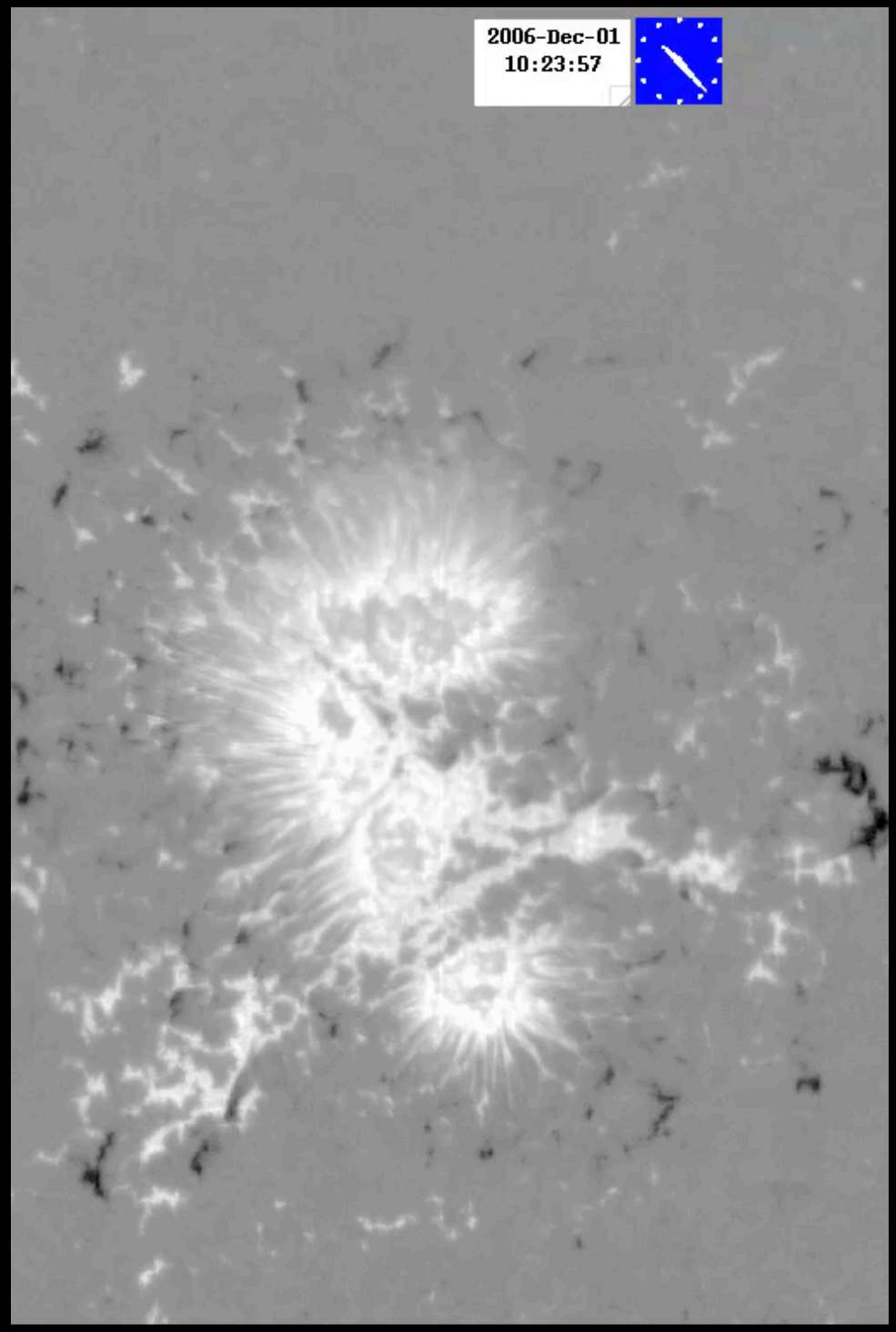

(Credit: Alan Title, LMSAL)

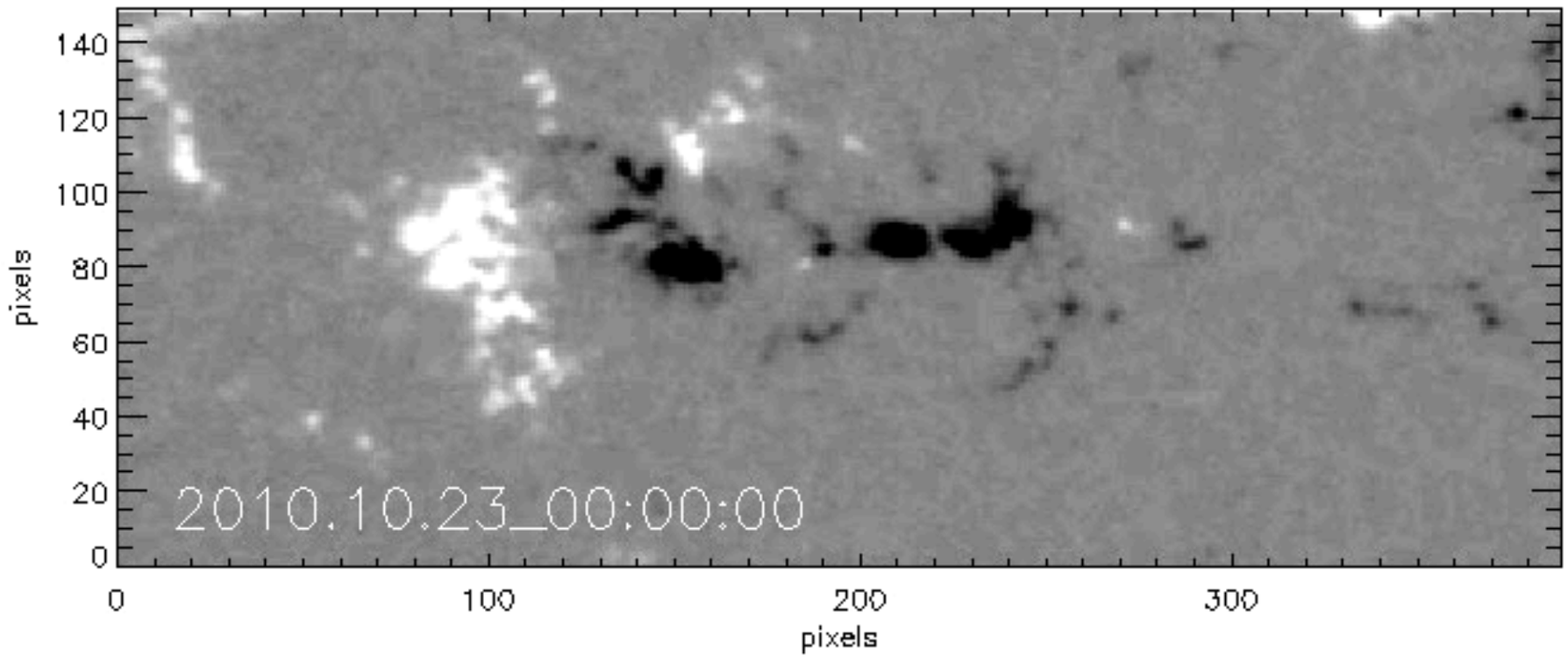

More examples of active regions

redit: Yang Liu,SDO/HMI/Stanford)

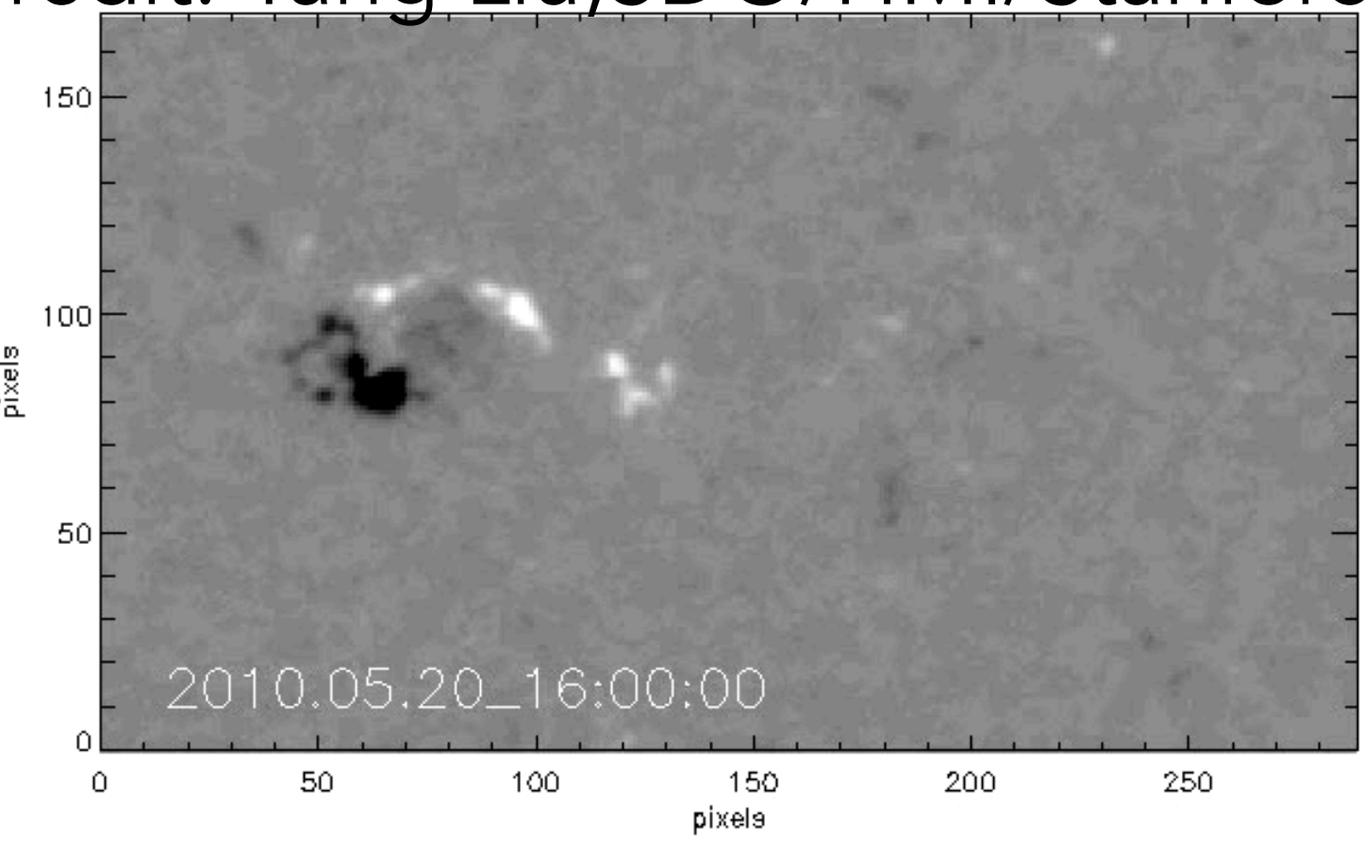

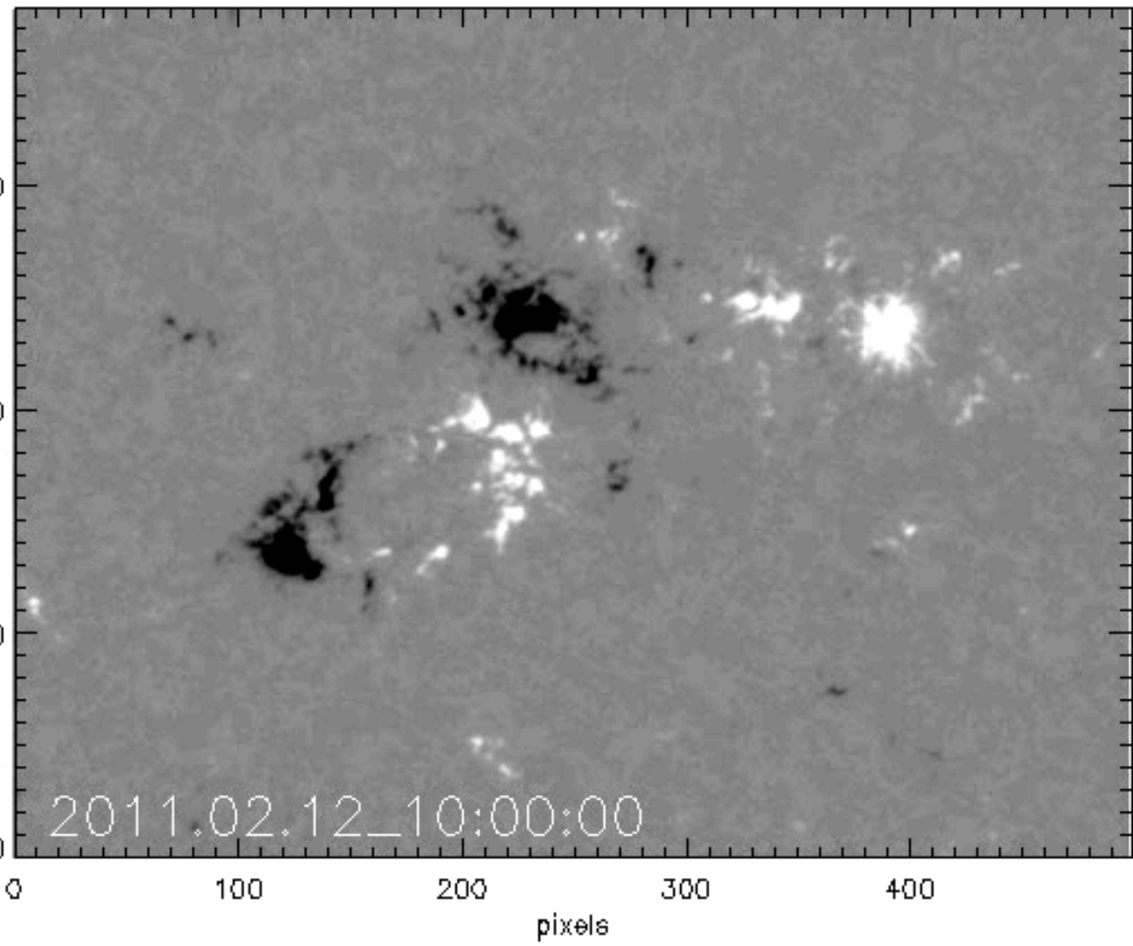

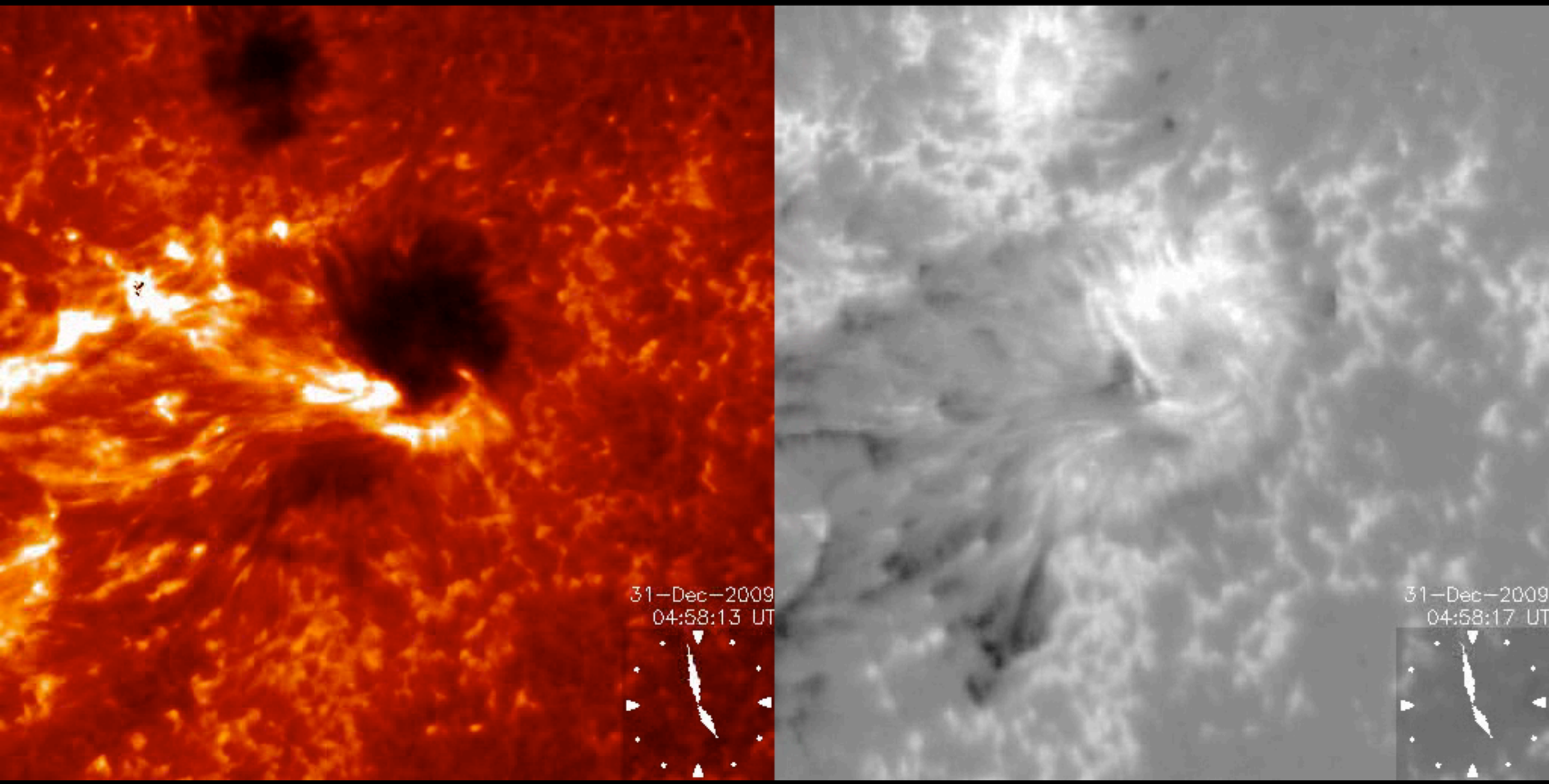

Hinode SOT observation of sunspot formation (Shimizu, Ichimoto & Suematsu 2012): A Ca II dark ring precedes appearance of the penumbra in G-band BFI images

Models of Sunspots as an Isolated Entity

- Sunspot as a steady state, vertically oriented magnetic flux tube (e.g. Schlüter & Temesvàry, 1958; Deinzer 1965).
- Sunspot as collection cluster of flux tubes (Parker 1979): argument based on force balance considerations (magnetic tension vs. buoyancy).
- **Jupyter Notebooks https://github.com/fluxtransport/HelioLectures/**
  - **sunspot_lecture_part1.ipynb**

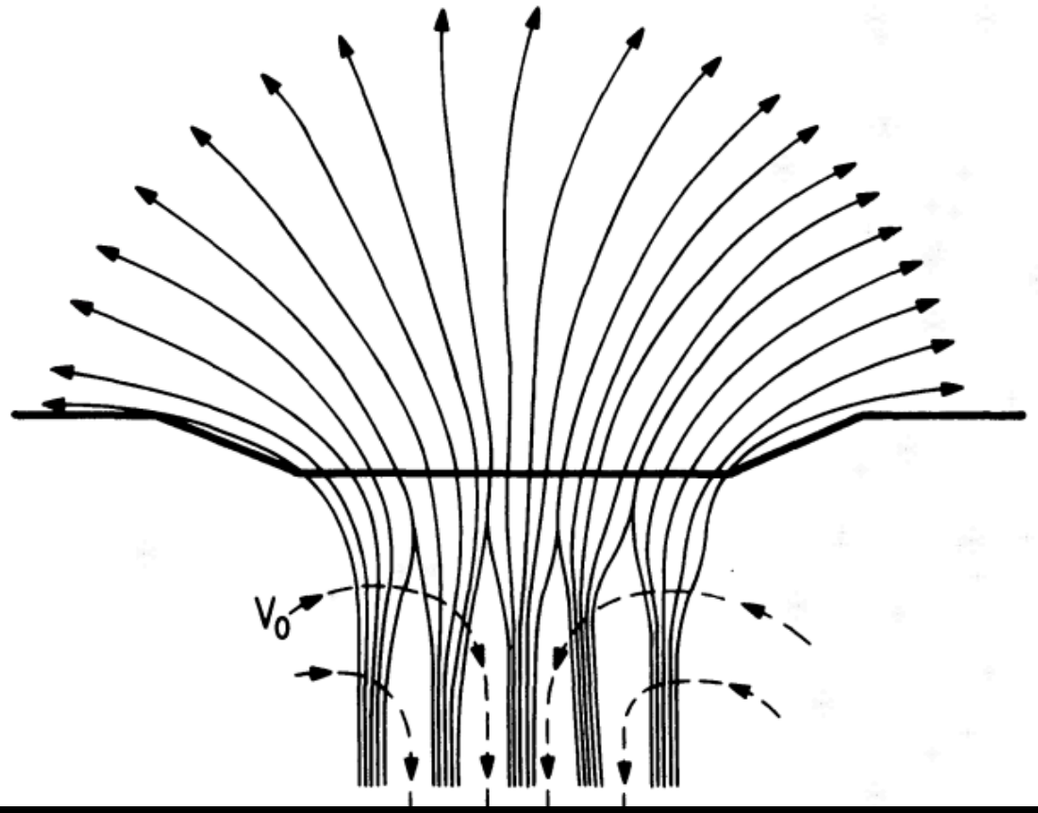

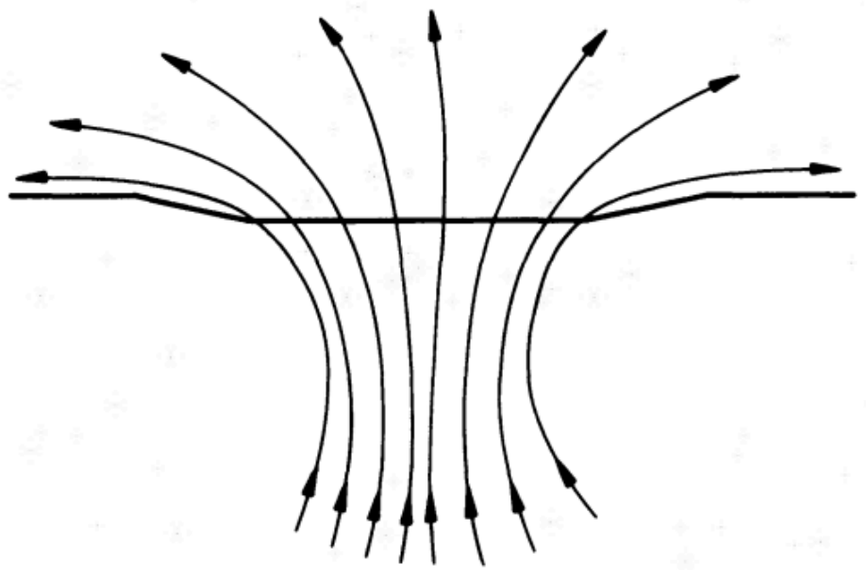

Some implications of the simplistic model

NB: This high β region umbra is an artifact of the simplistic model (axisymmetric, no flows).

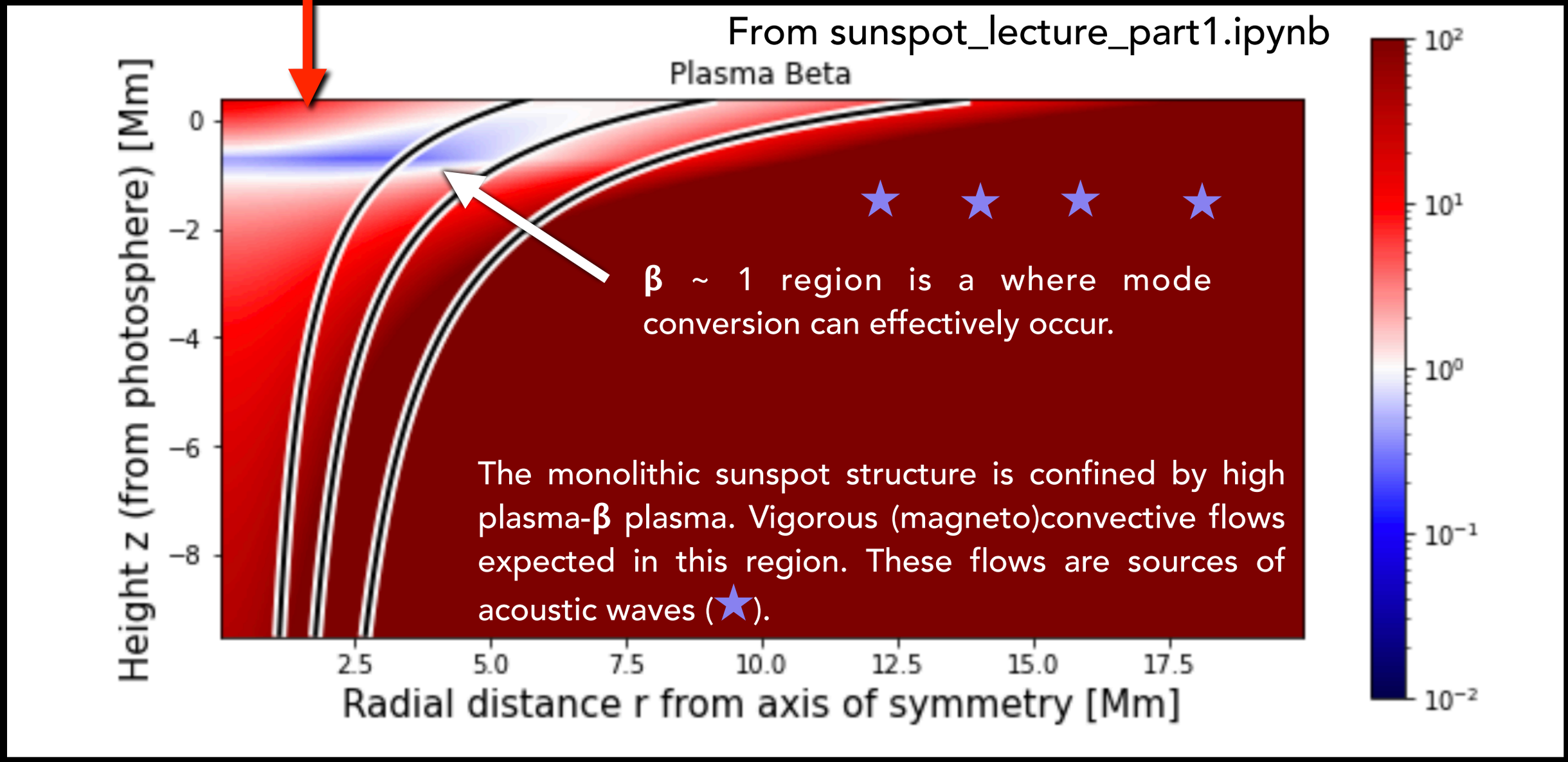

Cally, Crouch & Braun, 2003, MNRAS

Cameron, Gizon & Duvall, “Helioseismology of Sunspots”, 2008, Solar Physics

Nordlund, Stein & Asplund, “Solar Surface Convection”, 2009, Living Reviews in Solar Physics

Felipe, Khomenko & Collados, “Magnetoacoustic waves in sunspots …. “, 2010, ApJ

Khomenko & Collados, “Oscillations and Waves in Sunspots”, 2015, Living Reviews in Solar Physics

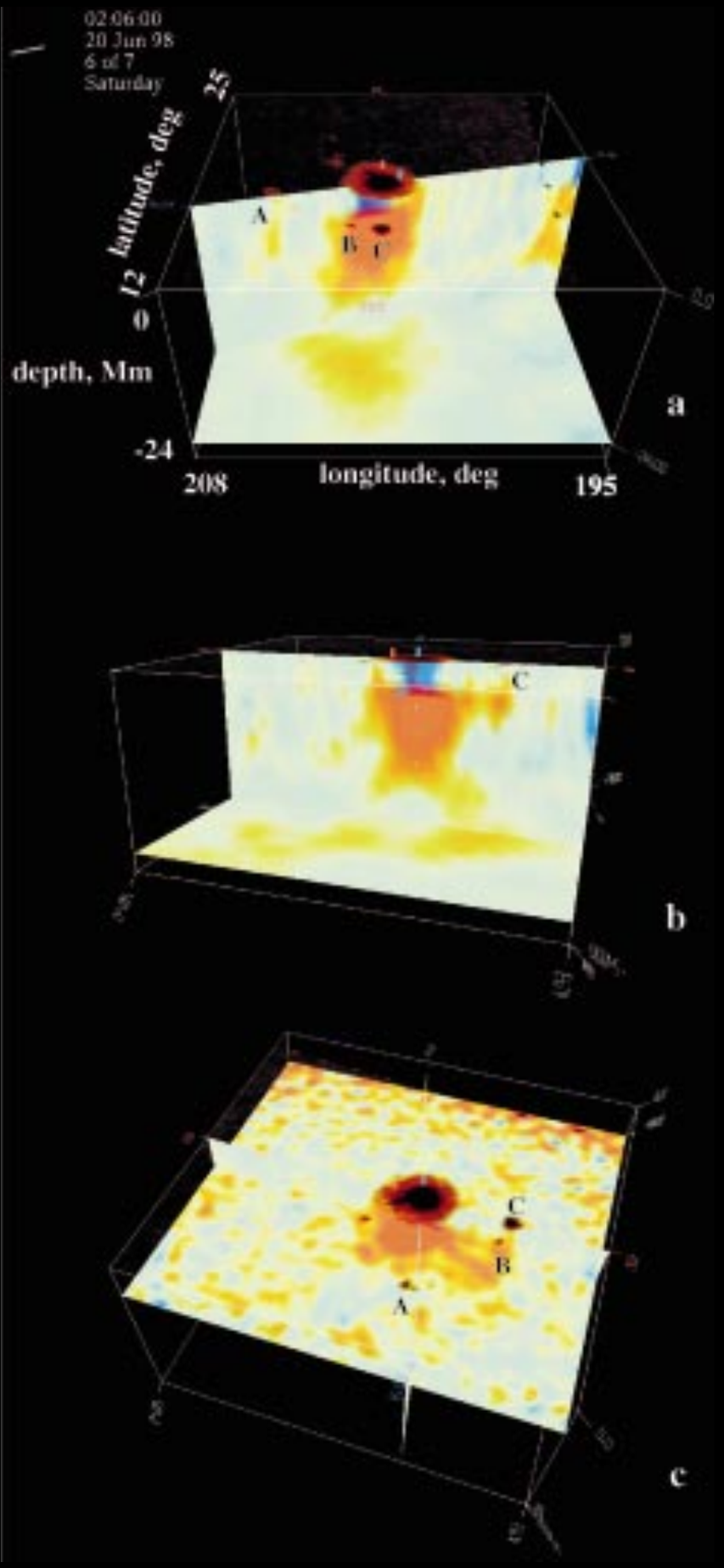

In Figure 8 we show (in three different projections) an example of the internal structure of a large sunspot observed on 17 June 1998. An image of the spot taken in the continuum is shown at the top. The wave-speed perturbations in the spot are much stronger than in the emerging flux. The typical perturbations range from 0.3 to 1 km s^{-1}. At a depth of 4 Mm, a 1 km s^{-1} wave-speed perturbation corresponds to a 10% temperature variation (about 2800 K) or to a 18 kG magnetic field. It is interesting that beneath the spot the perturbation is negative in the subsurface layers and becomes positive in the deeper interior. These data also show 'fingers'–narrow

Kosovichev, Duvall & Scherrer (2000, Solar Physics, 192, 159) reported results from time-distance helioseismology applied to SOHO/MDI Dopplergrams.

Based on work considering effect of magnetic fields (e.g. Schunker et al. 2013), these inversion results are **no longer believed** to be representative of actual sunspot subsurface structure. However …

Convection

Flux Emergence Model With Imposed Flux Rope

Cheung, Rempel, Title & Schüssler (2010)

- Kinematically advect a twisted semi-torus into the domain with an upflow speed of 1 km/s (Mach number approx. 0.03)
- Semi-major axis: R = 16 Mm
- Semi-minor axis: a = 3.6 Mm
- Dimensionless twist parameter $\lambda = 0.5$
- B = 21 kG (at tube axis), plasma $\beta = 26$
- Toroidal flux $\Phi = 7 \times 10^{21}$ Mx
- Mass injected = 1.4×10^{24} g = 40% of mass in domain
- Potential field at top boundary

$$
\begin{aligned}
\mathbf{B} &= \nabla \times [A_\phi(r,\theta)\hat{\phi}] + B_\phi(r,\theta)\hat{\phi}, \\
A_\phi(r,\theta) &= \frac{\lambda a^2 B_t}{2r\sin\theta} \exp\left\{\frac{-\varpi^2}{a^2}\right\}, \\
B_\phi(r,\theta) &= \frac{aB_t}{r\sin\theta} \exp\left\{\frac{-\varpi^2}{a^2}\right\}, \\
\varpi &= \sqrt{r^2 + R^2 - 2rR\sin\theta}.
\end{aligned}
$$

Following Fan & Gibson 2004

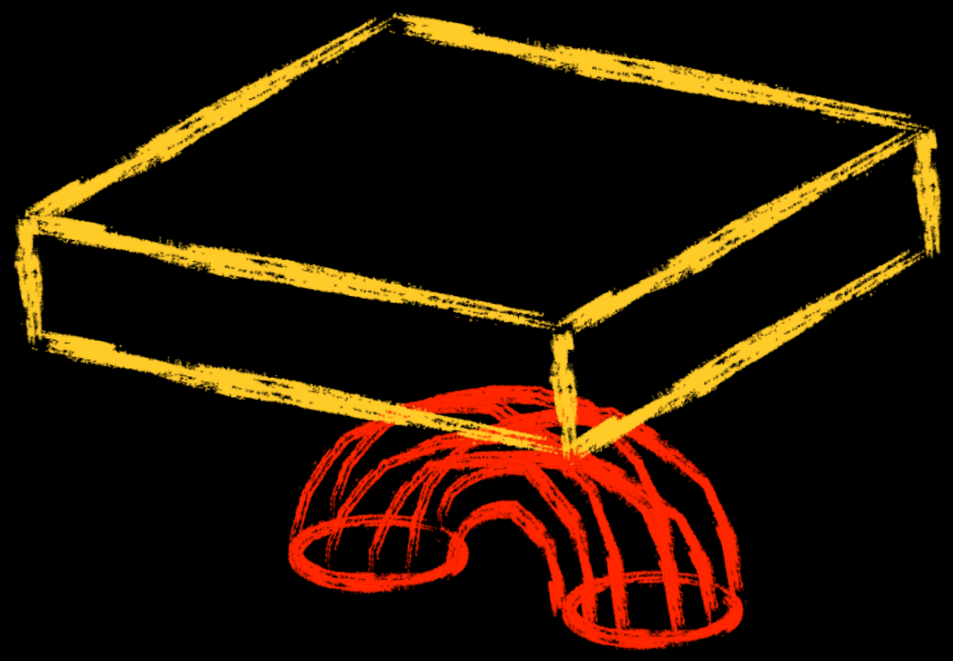

Radiative MHD simulation of AR formation

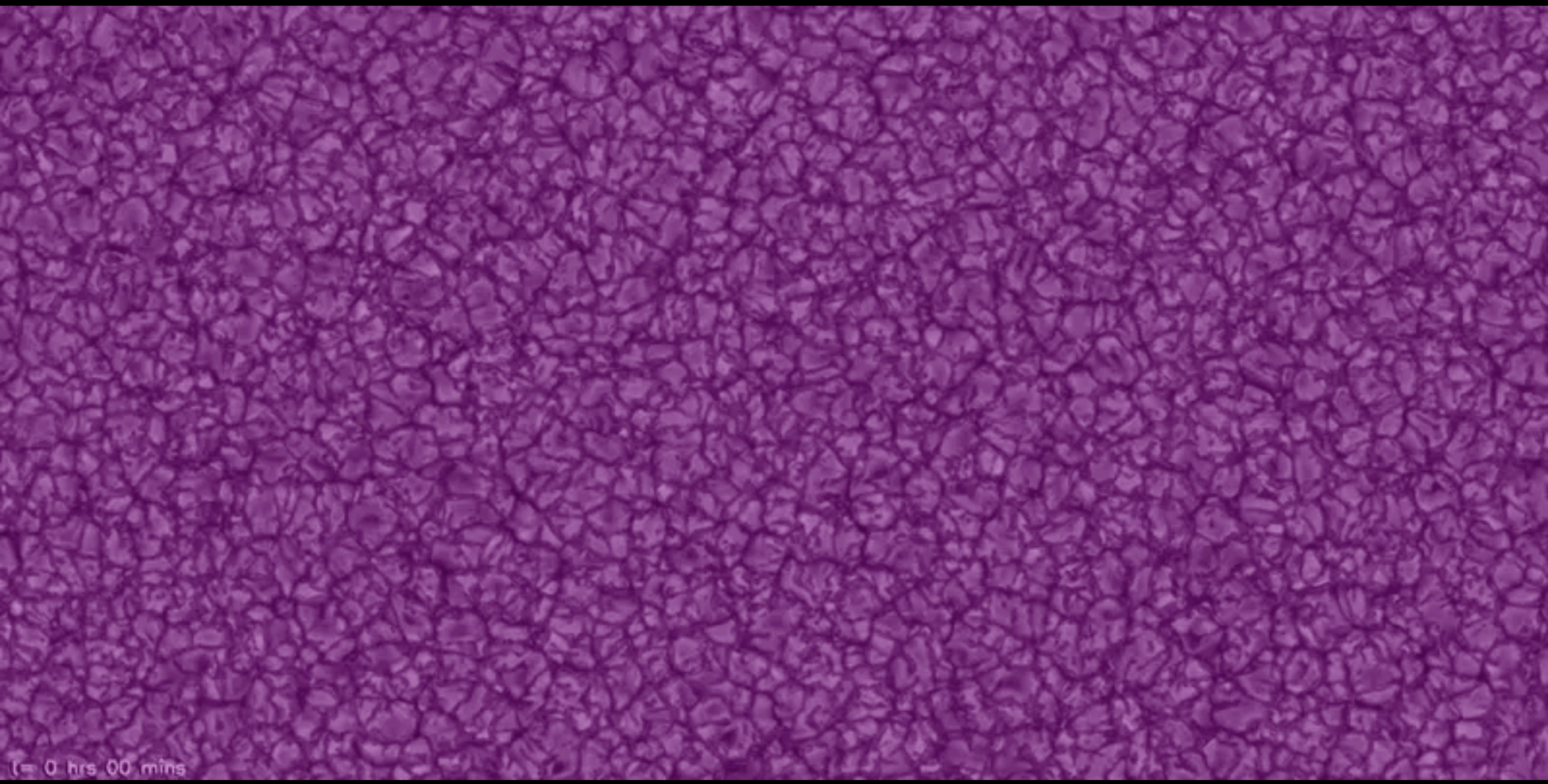

Cheung, Rempel, Title & Schüssler (2010)

Red (negative magnetic flux) Green (horizontal magnetic field) Blue (positive magnetic flux)

Purple background (brightness intensity of convective flows)

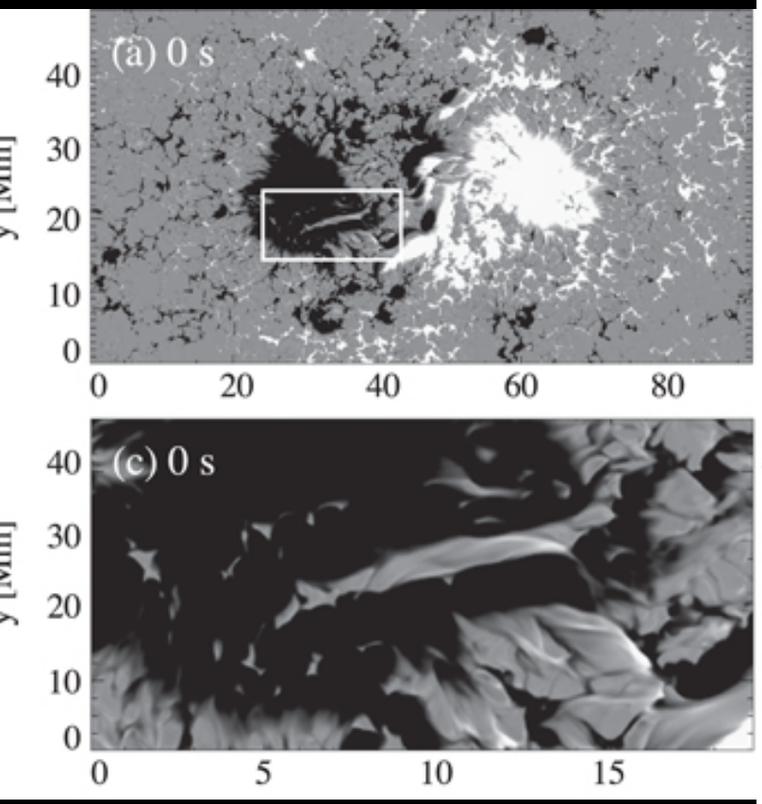

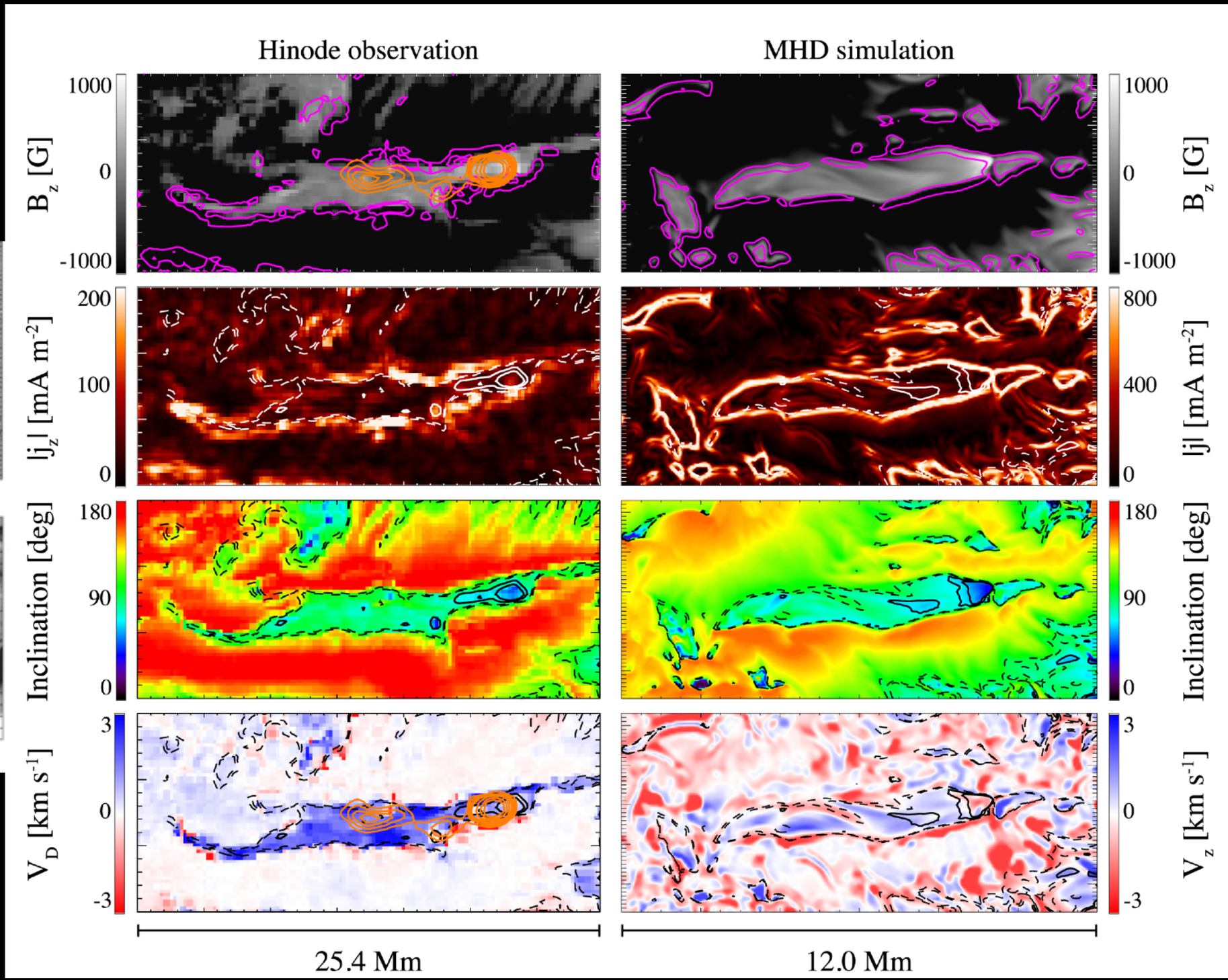

Toriumi, Cheung & Katsukawa (2015): Compared light bridge formed in MHD simulation (Cheung et al. 2010) with observed light bridge. Found general agreement in photospheric observables.

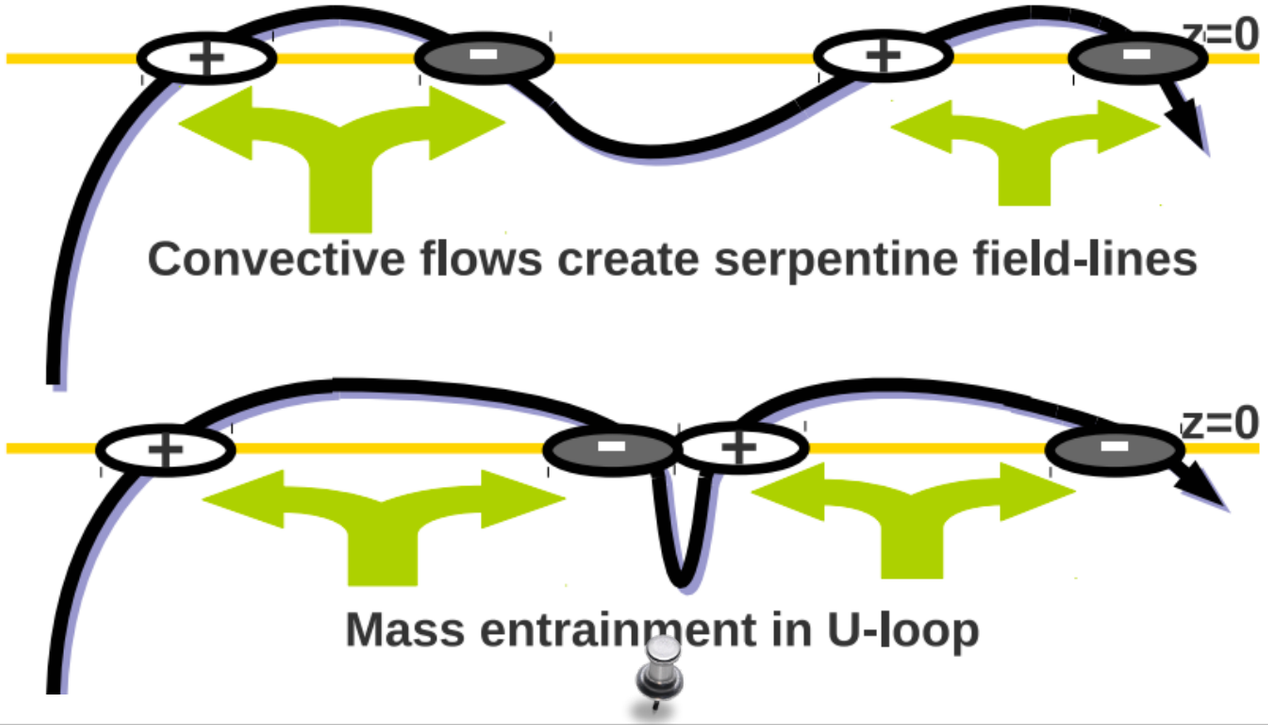

$$\frac{\partial \overline{\mathbf{B}}}{\partial t} = \nabla \times (\overline{\mathbf{v}} \times \overline{\mathbf{B}}) + \nabla \times E\,, \tag{34}$$

where $E = \overline{\mathbf{v}' \times \mathbf{B}'}$ is the (azimuthally-averaged) mean-field electromotive force resulting from correlations between the magnetic field and velocity field fluctuations (Krause and Rädler, 1980; Rädler, 1980). The time rate of change of magnetic flux crossing the circular surface $\mathcal{C}$ is then

$$\dot{\Phi}_{\mathcal{C}} = \int_{\mathcal{C}} \frac{\partial \overline{\mathbf{B}}}{\partial t} \cdot \mathbf{d}S = \oint_{\partial \mathcal{C}} \left(\overline{\mathbf{v}} \times \overline{\mathbf{B}} + E\right) \cdot \mathbf{d}l\,, \tag{35}$$

$$= \dot{\Phi}_{\rm m} + \dot{\Phi}_{\rm f}\,, \tag{36}$$

where

$$\dot{\Phi}_{\rm m} = 2\pi R [\overline{\mathbf{v}} \times \overline{\mathbf{B}}]_\theta = 2\pi R (\overline{v}_z \overline{B}_r - \overline{B}_z \overline{v}_r)\,, \tag{37}$$

$$\dot{\Phi}_{\rm f} = 2\pi R \mathcal{E}_\theta = 2\pi R \overline{v'_z B'_r - B'_z v'_r}\,. \tag{38}$$

Figure 37: Schematic drawing illustrating the effect of granular flows on magnetic polarities from a serpentine field line. Image reproduced with permission from Cheung *et al.* (2010), copyright by AAS.

Mass discharge

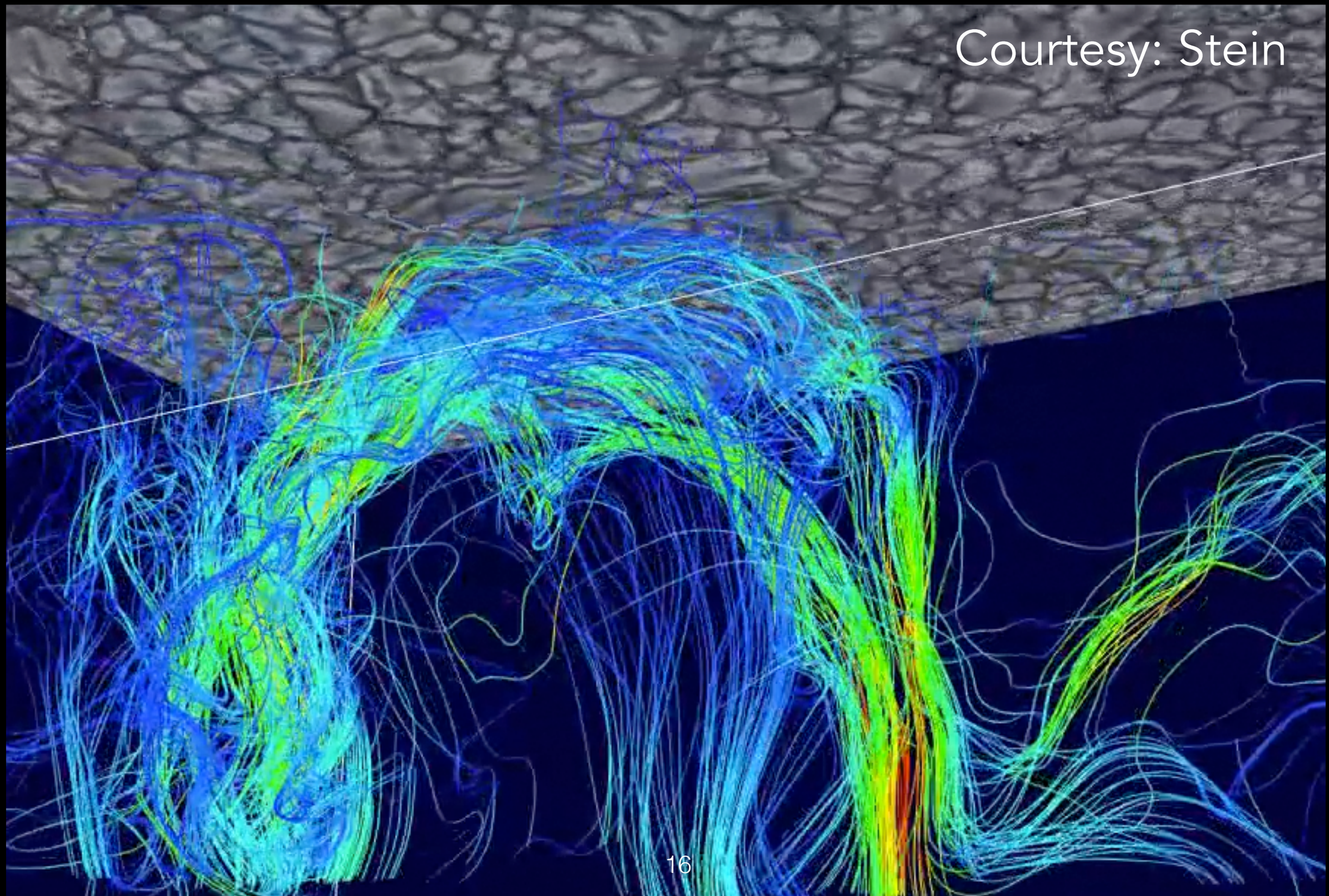

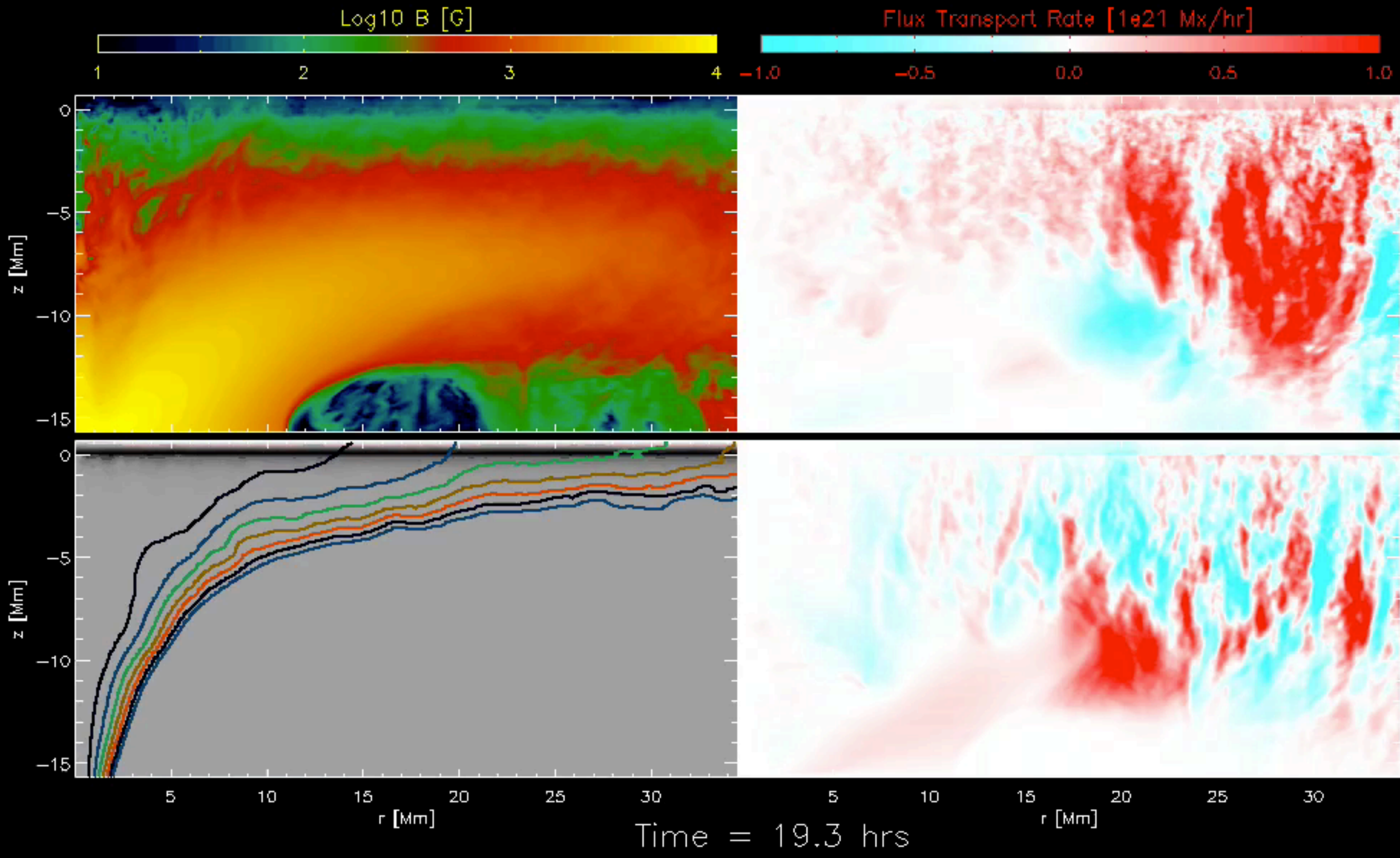

From simulation in Rempel & Cheung (2014). See also Hotta & Iijima (2020).

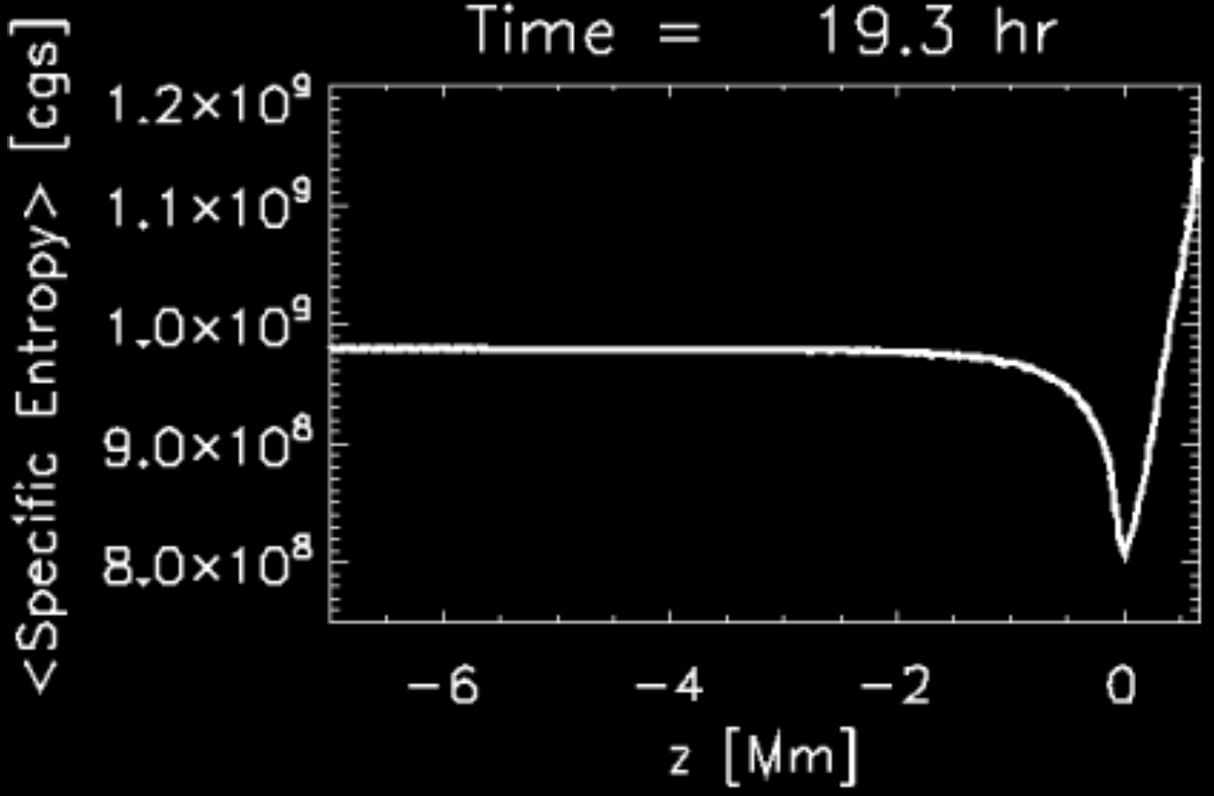

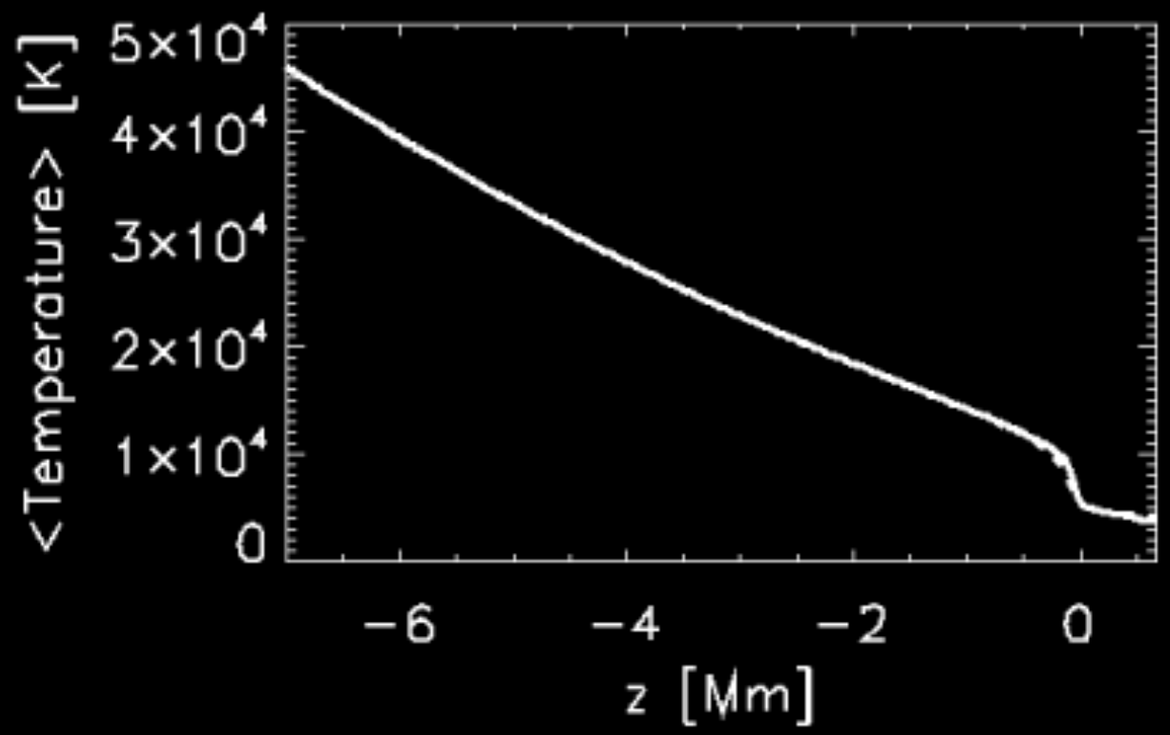

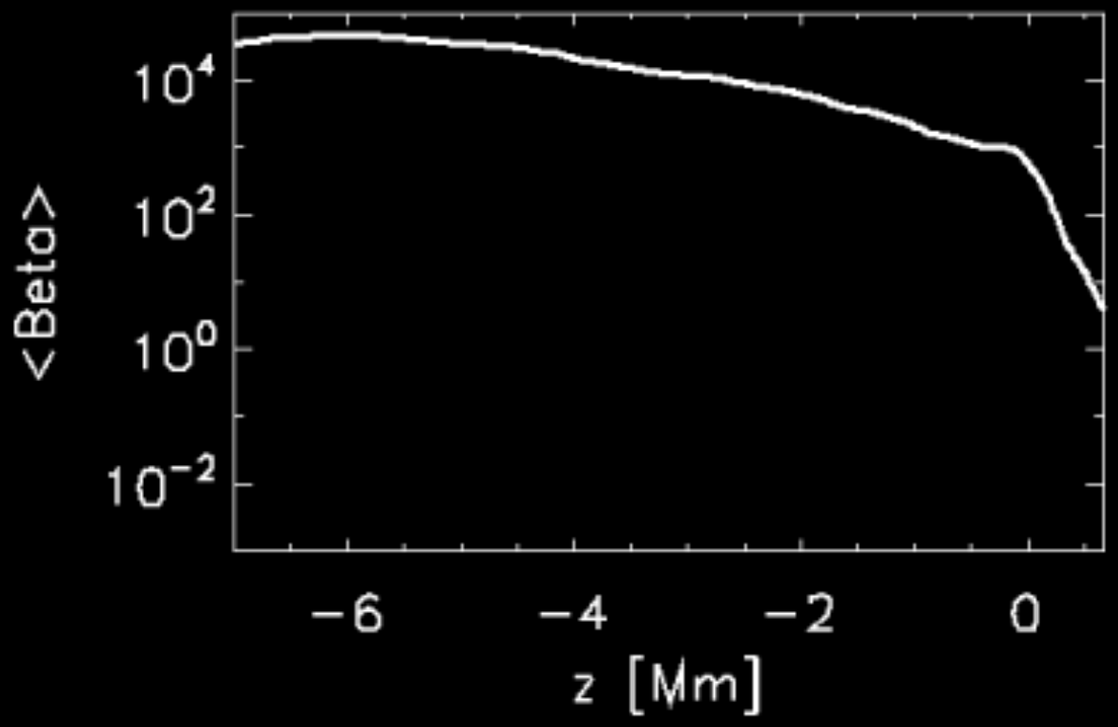

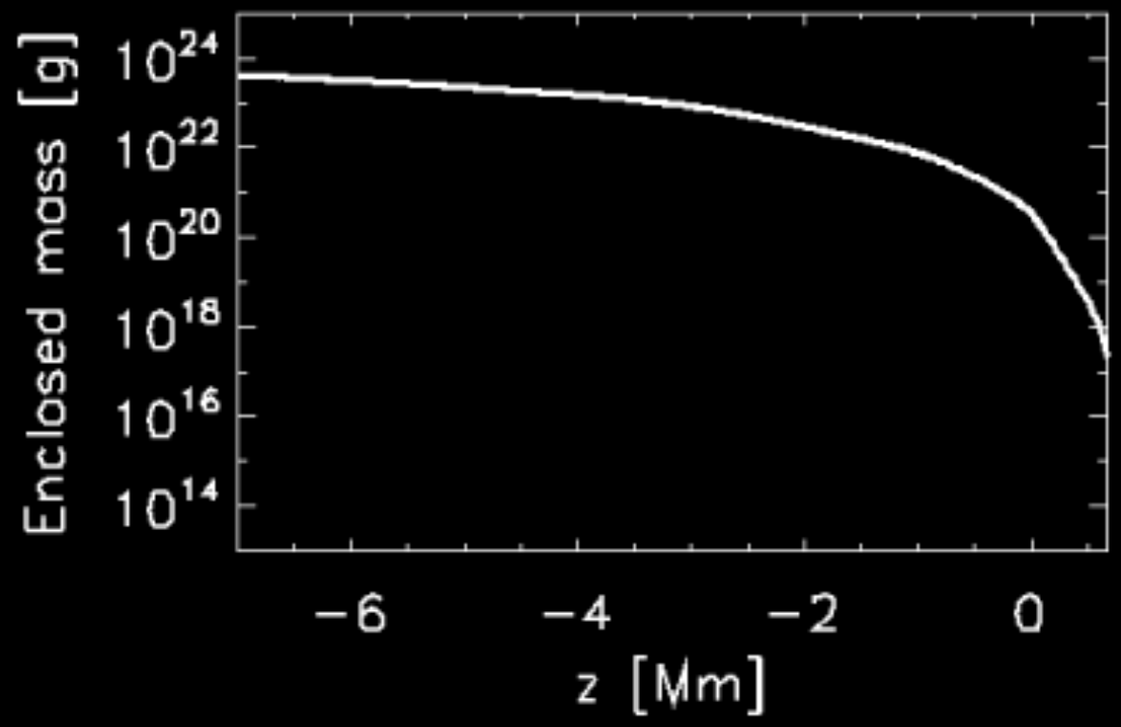

Solid lines: Quantities enclosed by 8×10^{20} Mx flux surface

Rempel & Cheung (2014)

Mean Flows

Correlations

Mean Flows + Correlations

Flux Transport Rate [1e20 Mx/hour]

6
4
2
0
-2
-4
-6

Time [hours]

120
100
80
60
40
20

Flux transport due to horizontal flows

Flux transport due to vertical flows

Flux transport due to both horizontal and vertical flows

Flux Content

r [Mm]

5 10 15 20 25 30

ϕ dot x4

Flux Spreading in the Decay Phase

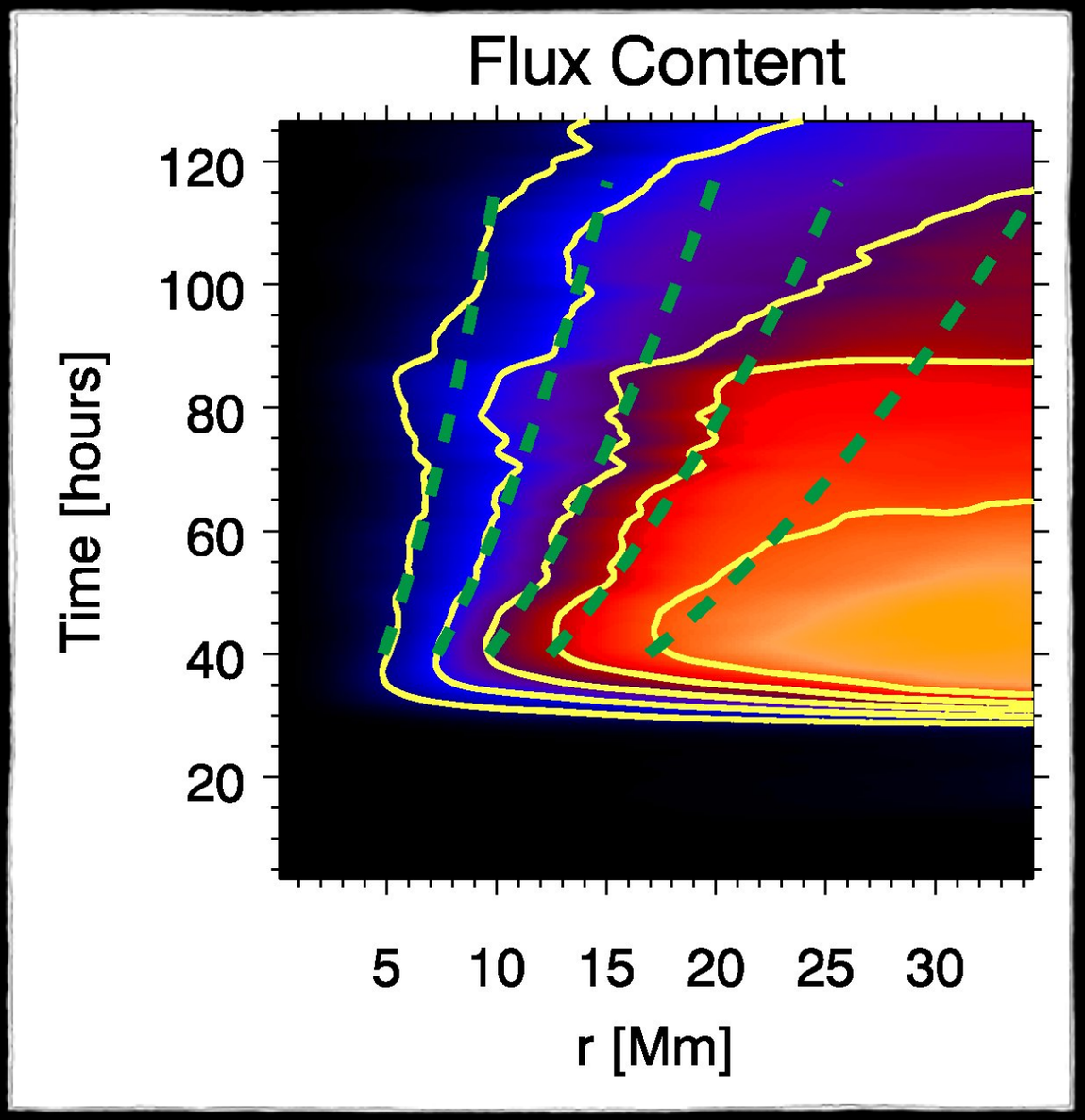

Decay due to turbulent diffusion (see Meyer et al 1974 and Mosher 1977)

$$B_z(r,t) = \frac{\Phi_0}{\pi\sigma(t)^2} e^{-r^2/\sigma(t)^2}, \text{ where}$$

$$\sigma(t) = \sqrt{\sigma_0^2 + 4\eta_{\text{turb}} t}.$$

Green dashed lines show the self-similar solution for:

Φ_0 = 1.1 x 10^{22} Mx,

σ_0 = 11 Mm, and

η_{Turb} = 350 $km^2 s^{-1}$.

Yellow contours show surfaces of constant enclosed flux in intervals of 2x10^{21} Mx (for the leading polarity).

Hotta & Iijima (2020): Sunspot Formation & Decay in simulation covering entire CZ

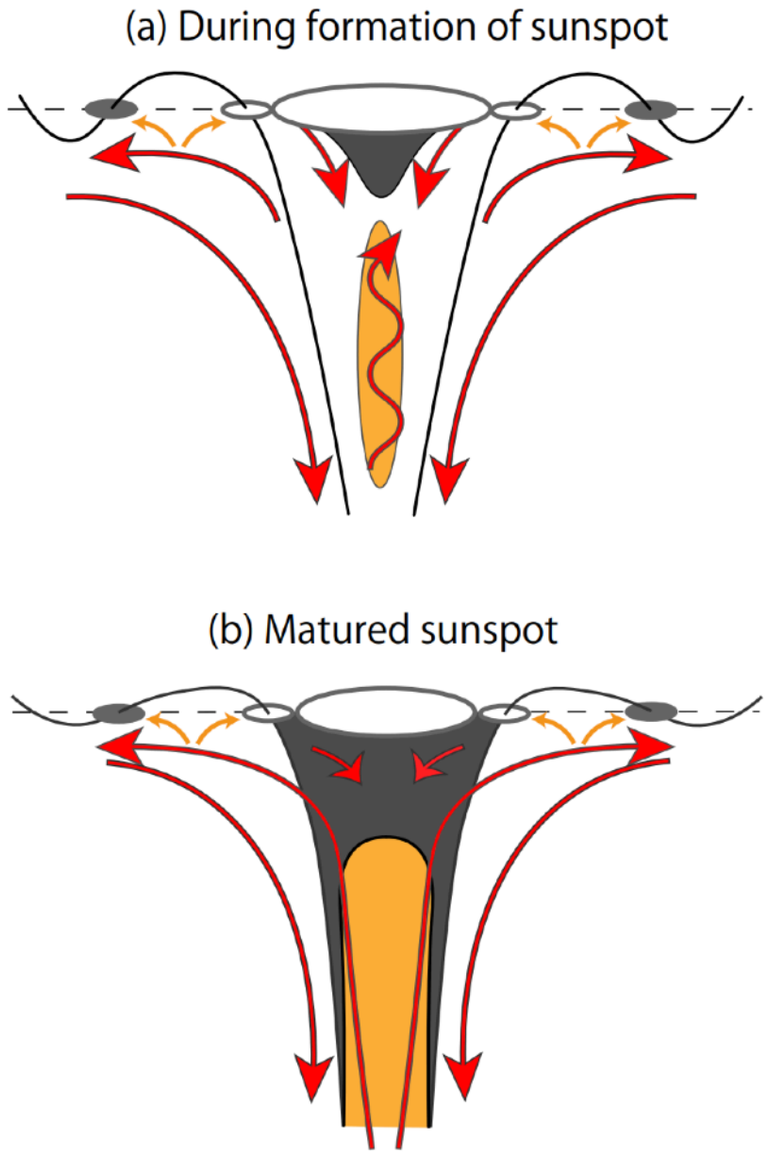

Figure 21. The summary of the sunspot structure during formation (panel a) and the matured sunspot (panel b). The red arrows show the coherent mean flow, and the orange arrows show the turbulent flow, which contributes to the collection of the magnetic flux. The black and orange areas correspond to low and high temperatures, respectively.

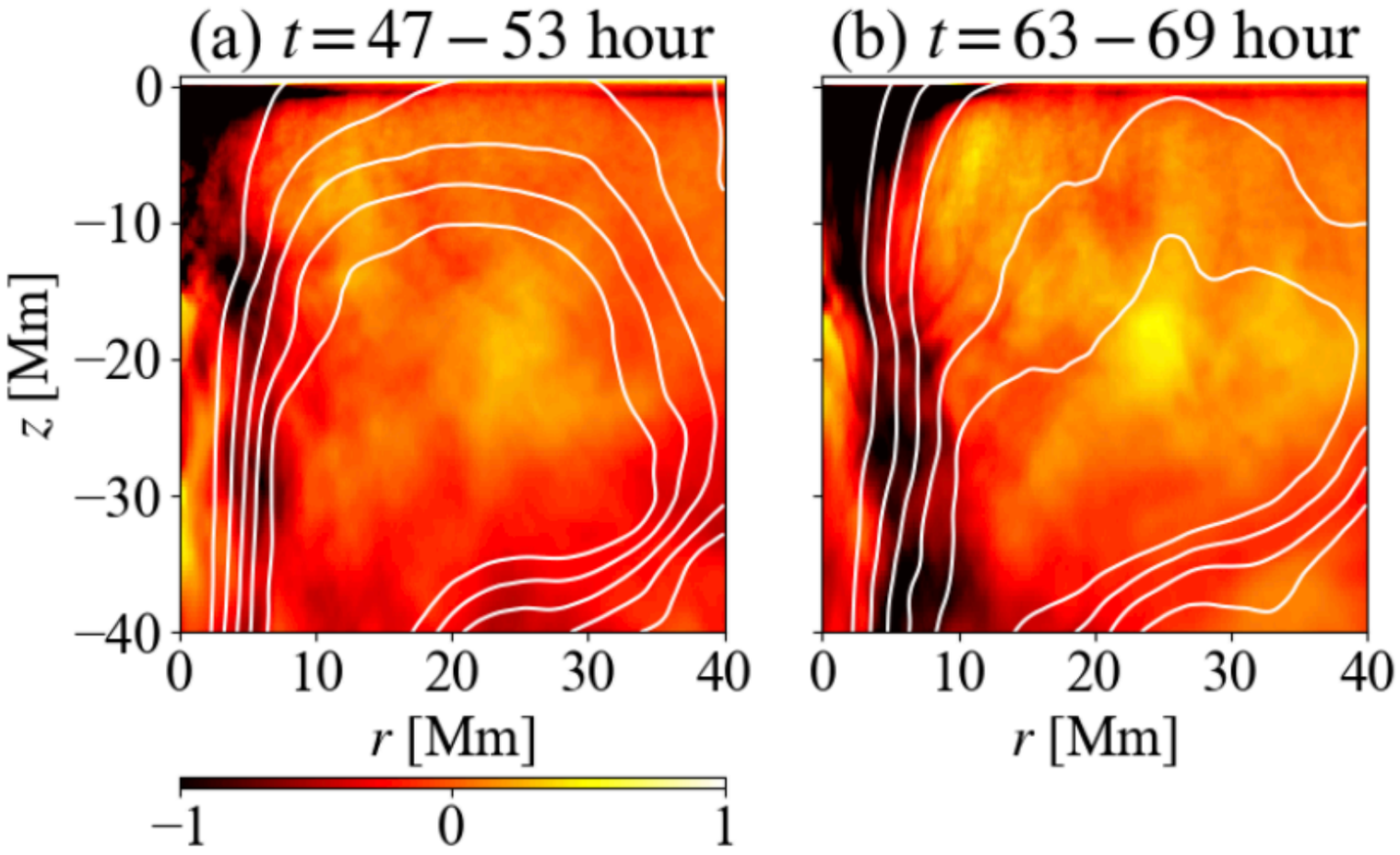

Figure 20. Azimuthally averaged normalized temperature $\tilde{T}$ is shown. Panels a and b show the average value in t = 47 and 53 hr (during the sunspot formation) and t = 63 and 69 hr (matured sunspot), respectively.

Magnetic flux concentrations from turbulent stratified convection*

P. J. Käpylä[1,2,3], A. Brandenburg[3,4,5,6], N. Kleeorin[7,3], M. J. Käpylä[1] and I. Rogachevskii[7,3]

Received: 12 November 2015 **Accepted:** 20 December 2015

Abstract

Context. The formation of magnetic flux concentrations within the solar convection zone leading to sunspot formation is unexplained.

Aims. We study the self-organization of initially uniform sub-equipartition magnetic fields by highly stratified turbulent convection.

Methods. We perform simulations of magnetoconvection in Cartesian domains representing the uppermost 8.5–24 Mm of the solar convection zone with the horizontal size of the domain varying between 34 and 96 Mm. The density contrast in the 24 Mm deep models is more than 3×10^3 or eight density scale heights, corresponding to a little over 12 pressure scale heights. We impose either a vertical or a horizontal uniform magnetic field in a convection-driven turbulent flow in set-ups where no small-scale dynamos are present. In the most highly stratified cases we employ the reduced sound speed method to relax the time step constraint arising from the high sound speed in the deep layers. We model radiation via the diffusion approximation and neglect detailed radiative transfer in order to concentrate on purely magnetohydrodynamic effects.

Results. We find that super-equipartition magnetic flux concentrations are formed near the surface in

or a horizontal uniform magnetic field in a convection-driven turbulent flow in set-ups where no small-scale dynamos are present. In the most highly stratified cases we employ the reduced sound speed method to relax the time step constraint arising from the high sound speed in the deep layers. We model radiation via the diffusion approximation and neglect detailed radiative transfer in order to concentrate on purely magnetohydrodynamic effects.

Results. We find that super-equipartition magnetic flux concentrations are formed near the surface in cases with moderate and high density stratification, corresponding to domain depths of 12.5 and 24 Mm. The size of the concentrations increases as the box size increases and the largest structures (20 Mm horizontally near the surface) are obtained in the models that are 24 Mm deep. The field strength in the concentrations is in the range of 3–5 kG, almost independent of the magnitude of the imposed field. The amplitude of the concentrations grows approximately linearly in time. The effective magnetic pressure measured in the simulations is positive near the surface and negative in the bulk of the convection zone. Its derivative with respect to the mean magnetic field, however, is positive in most of the domain, which is unfavourable for the operation of the negative effective magnetic pressure instability (NEMPI). Simulations in which a passive vector field is evolved do not show a noticeable difference from magnetohydrodynamic runs in terms of the growth of the structures. Furthermore, we find that magnetic flux is concentrated in regions of converging flow corresponding to large-scale supergranulation convection pattern.

Conclusions. The linear growth of large-scale flux concentrations implies that their dominant formation process is a tangling of the large-scale field rather than an instability. One plausible mechanism that can explain both the linear growth and the concentration of the flux in the regions of converging flow pattern is flux expulsion. A possible reason for the absence of NEMPI is that the derivative of the effective magnetic pressure with respect to the mean magnetic field has an unfavourable sign. Furthermore, there may not be sufficient scale separation, which is required for NEMPI to work.

A Simple Model by Longcope & Welsch (2000)

- "Current shunting" model for twisted active region emergence
- Idealized emerging active region has net twist
- Matched to force-free coronal field
- At the interface (photosphere), a horizontally diverging current drives a torque, which sends a torsional Alfvén wave down the tube.
- Over an Alfvén crossing time ~ 1 day (100 Mm @ 1 km/s), the tube unwinds while the coronal field is twisted up.

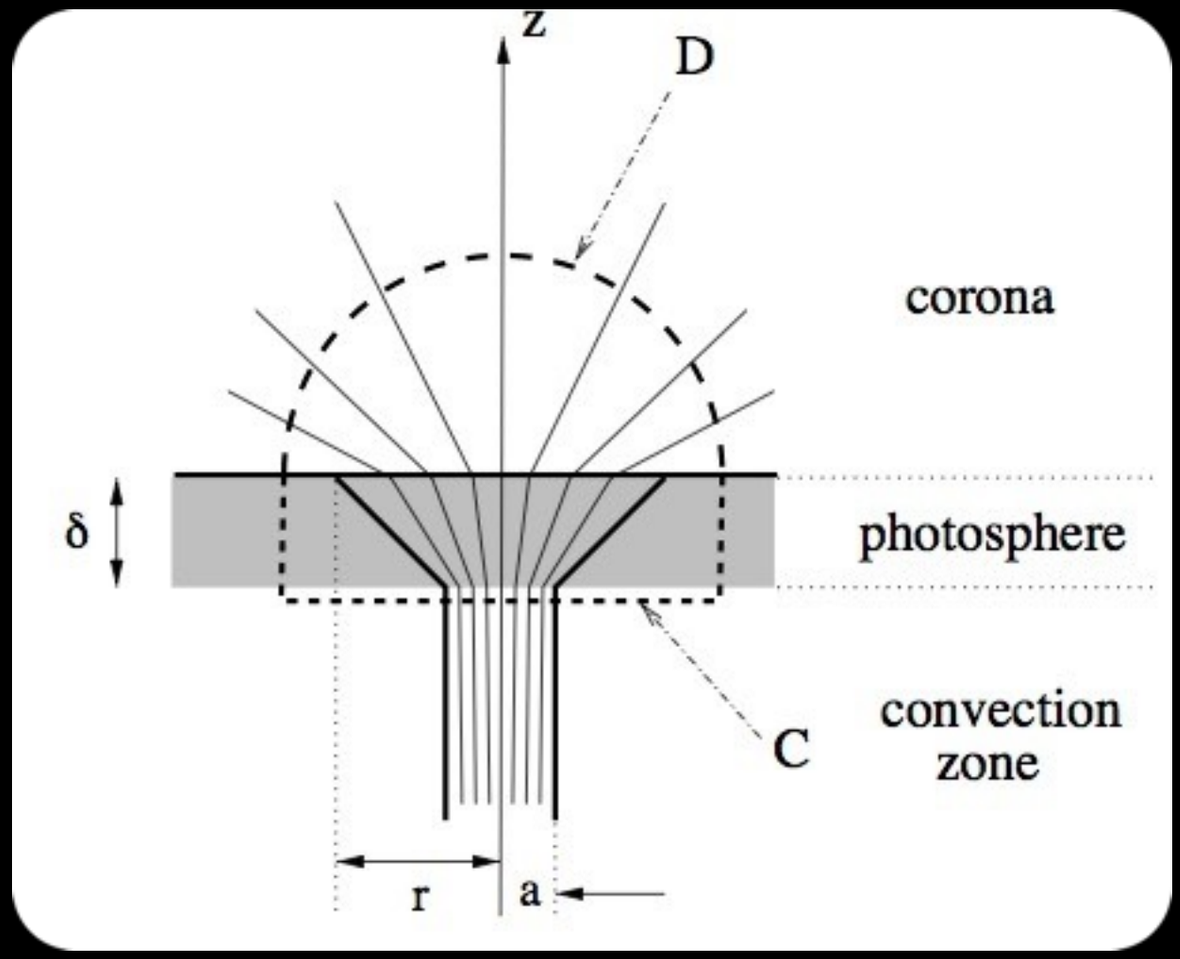

Exercise: show that a magnetic torque cannot be balanced by the gas pressure force. (hint: Sturrock, Hood & Archontis 2015)

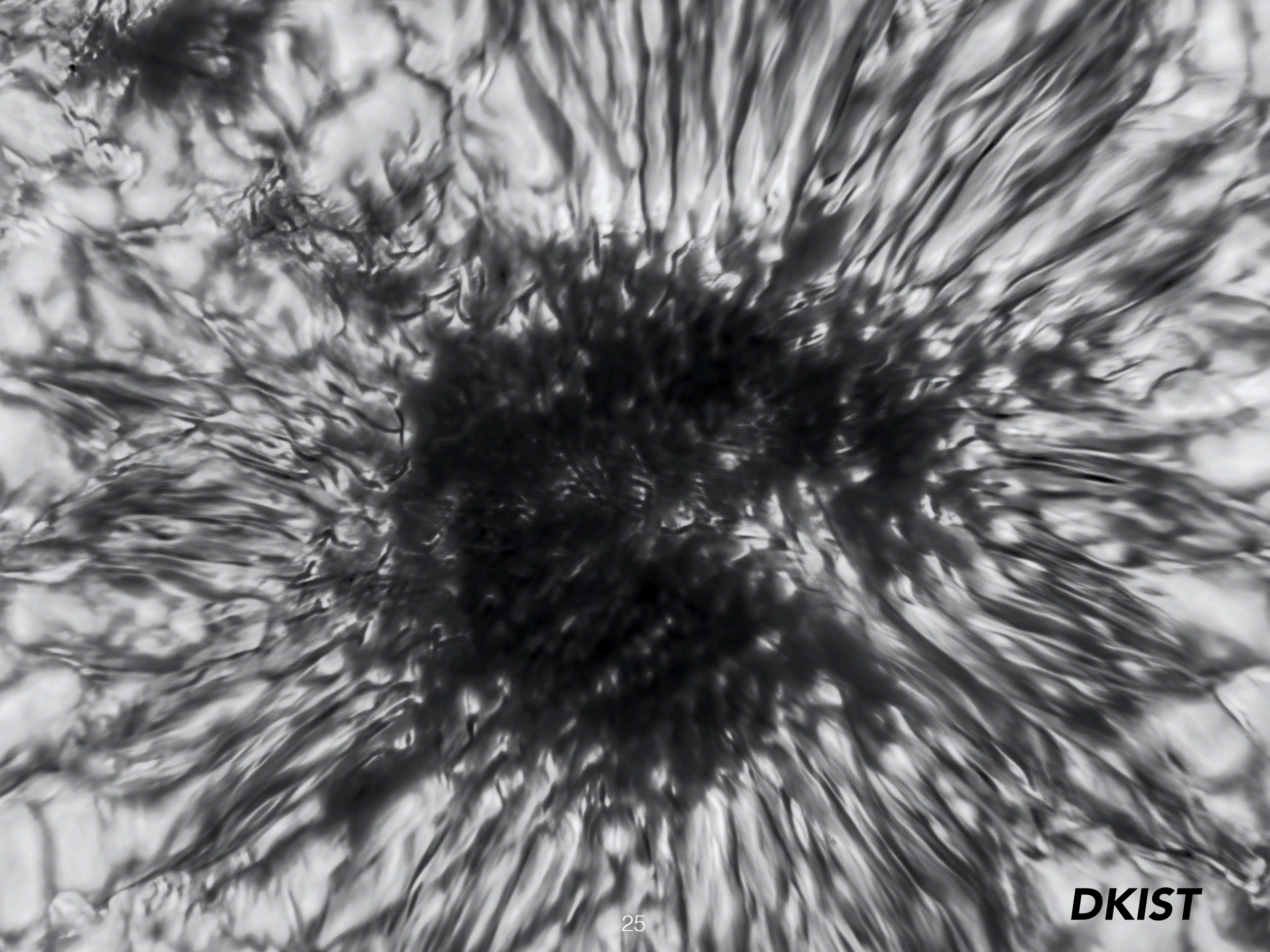

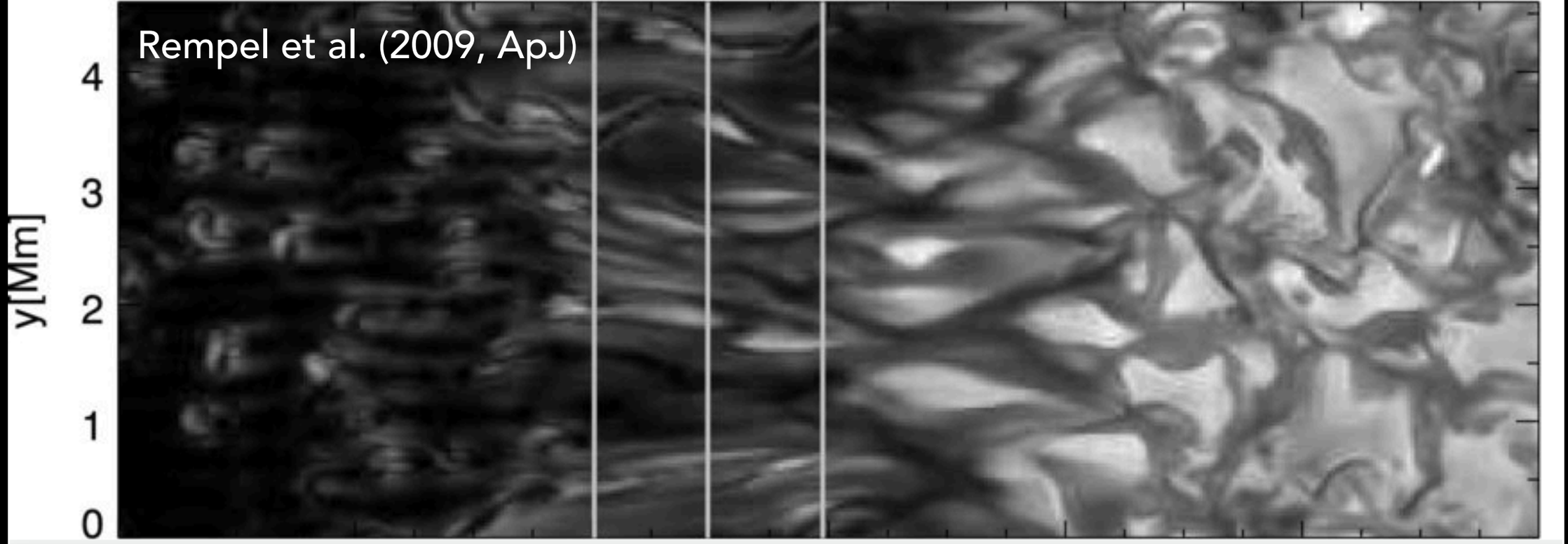
Rempel et al. (2009, ApJ)
y[Mm]
4
3
2
1
0

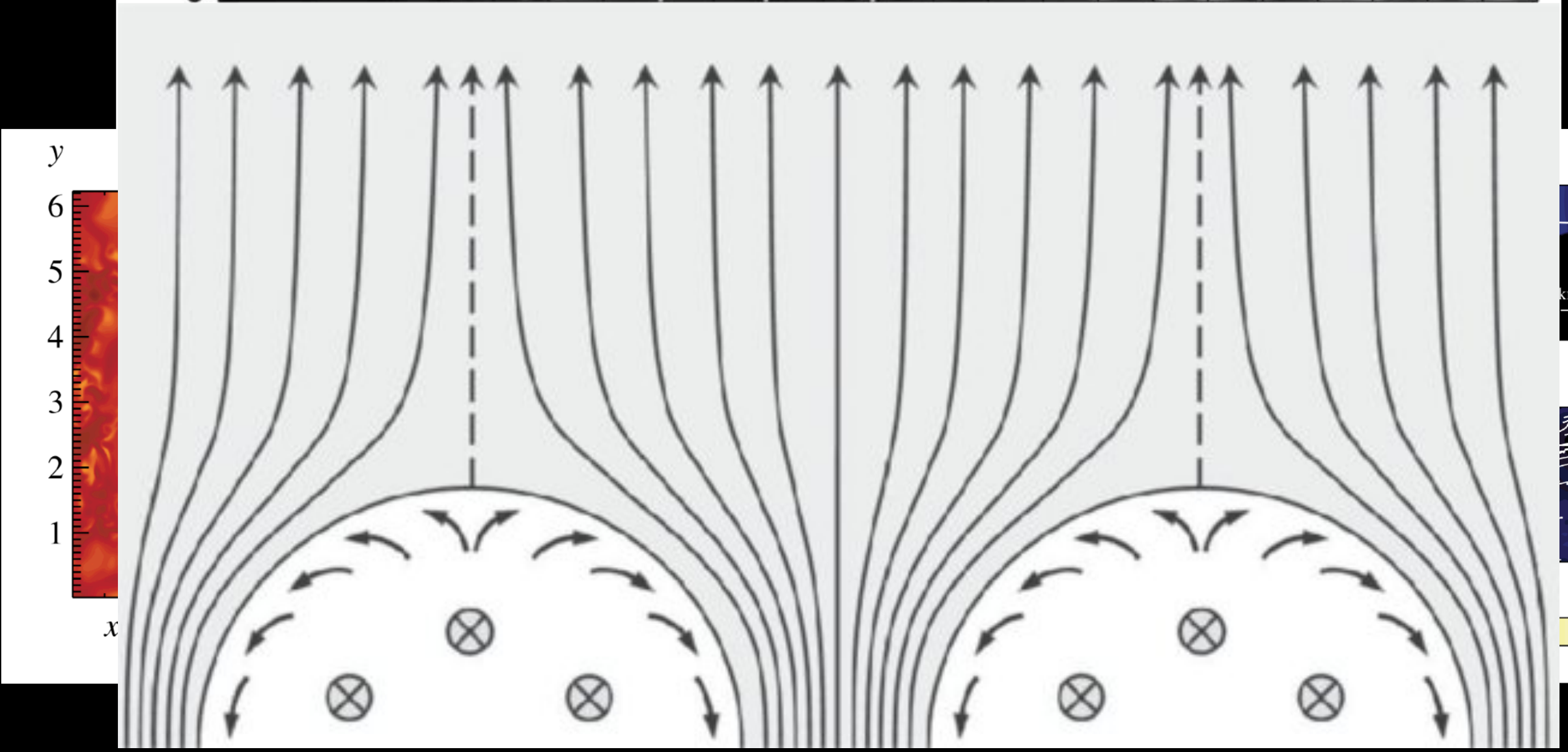
y
6
5
4
3
2
1
x
km/s
12

Fine structure of sunspots in Radiative MHD Simulations

- Rempel, Schüssler, Cameron & Knölker (2009, Science)

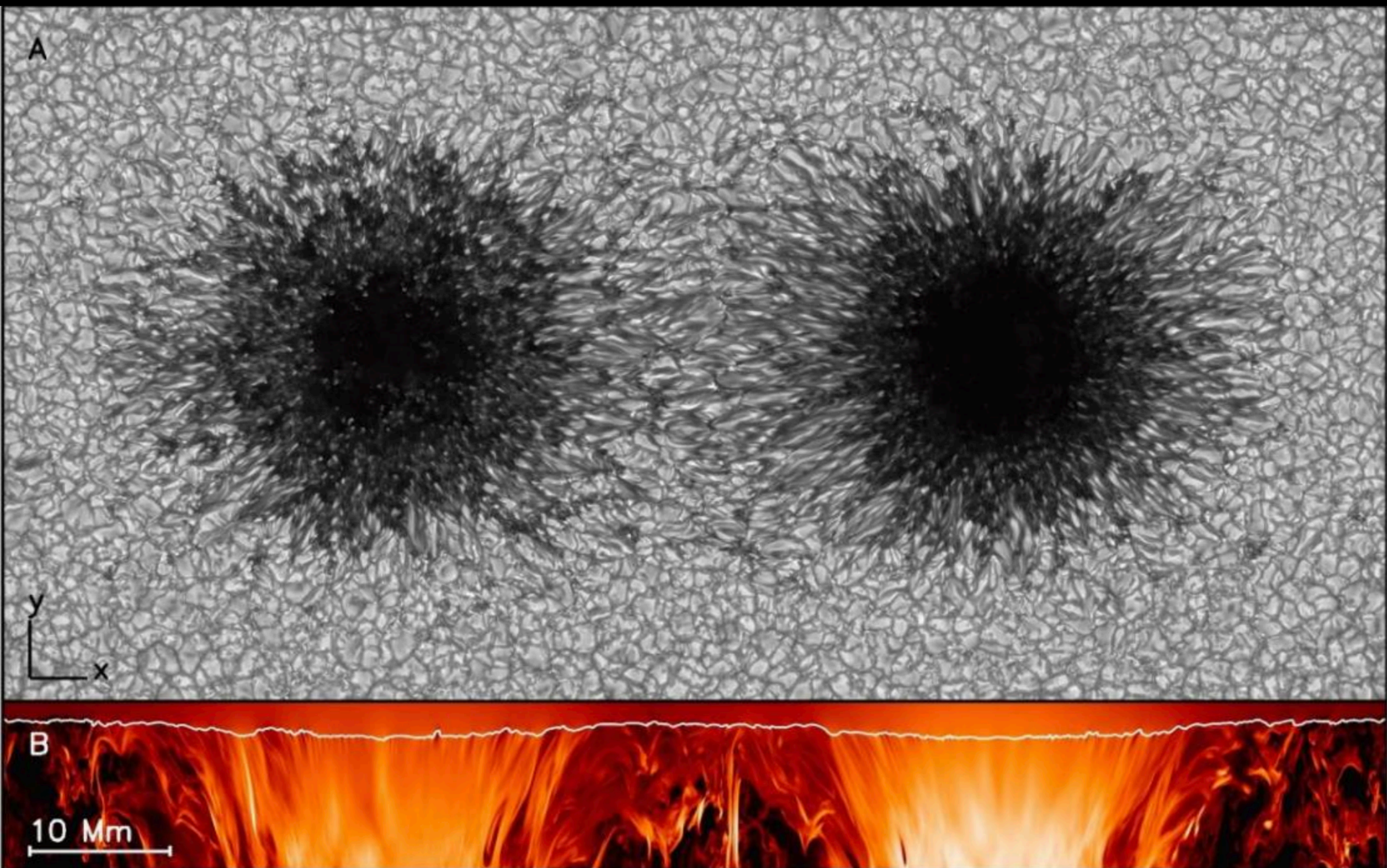

Fine structure of sunspots in Radiative MHD Simulations

- Rempel, Schüssler, Cameron & Knölker (2009, ApJ):
- Rempel (2011, ApJ): *"In the uppermost few 100 km, fast outflows are driven primarily through the horizontal component of the Lorentz force, which is confined to narrow boundary layers beneath* $\tau = 1$*"*
- Rempel (2012, ApJ): 3D simulation of a round sunspot with fully-fledge penumbra. The top boundary condition imposed a horizontal field that is 2x that of a potential field.
  - *Conclusion: sunspot subsurface akin to monolithic model*
  - **Jupyter Notebooks https://github.com/fluxtransport/HelioLectures/sunspot_lecture_part2.ipynb**

Fine structure of sunspots in Radiative MHD Simulations

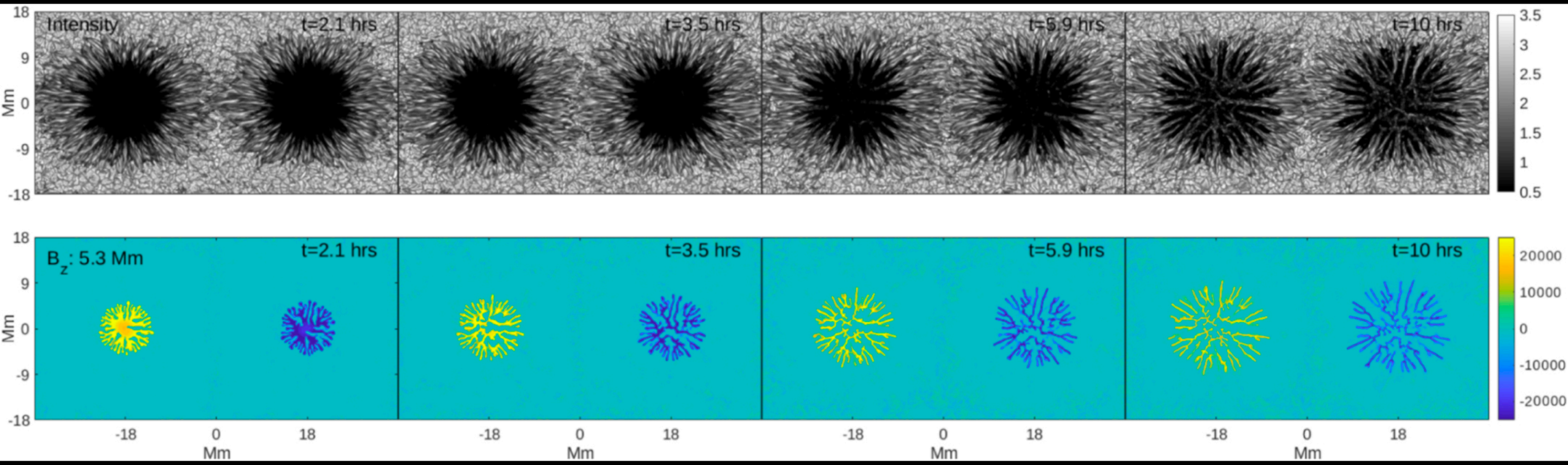

- Panja, Cameron & Solanki (2021): Slab-like geometry, with parameter study of expansion factor of then “valley”.
  - Higher expansion rate from CZ to photosphere creates more pronounced penumbral filaments
  - Evidence of the fluting instability (cf Parker 1979).
  - *Conclusion: subsurface structure consistent with cluster model.*

Confronting simulations with observations

- Jurčák et al. (2020): report discrepancies between models and observations, in terms of B at penumbral/umbral boundary, radial profile of B, and more.

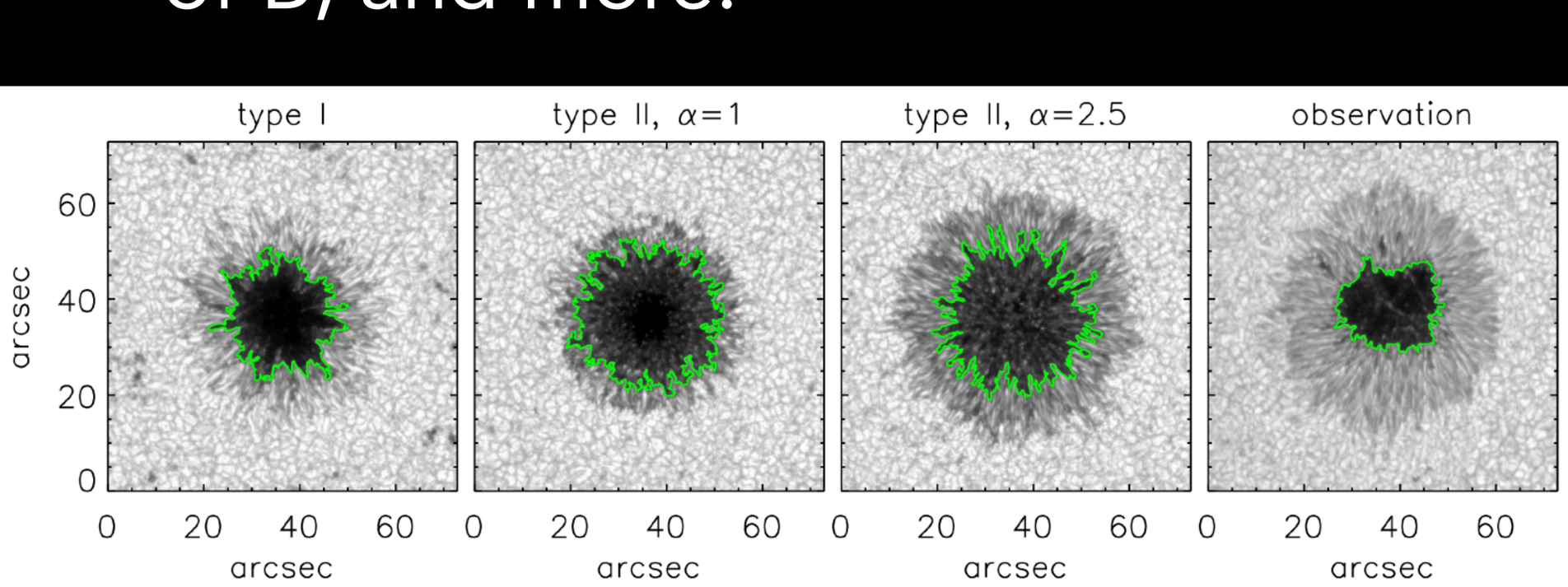

Fig. 4. Continuum intensity maps at 630.1 nm for analysed snapshots of simulated sunspots (degraded to the Hinode-like SP observations) and for an observed sunspots with comparable Φ. The green contours mark the UP boundary defined at $0.5 I_c^{QS}$.

Summary

- Types of sunspot models:
  1. (Semi-)analytical models of axisymmetric sunspots in time-independent state
  2. Linearized MHD models investigating wave propagation and mode conversion: see Khomenko & Collados review
  3. Radiative MHD simulations with imposed initial sunspot subsurface structure: e.g. Rempel (2011 papers, 2012)
  4. Radiative MHD simulations of active region formation (but no fully-fledged penumbrae): see also Stein & Nordlund (2013), Chen, Rempel & Fan (2017), Toriumi & Hotta (2019).
- Side messages:
  - Sunspot fields suck acoustic energy via mode conversion.
  - Observable consequences include chromospheric shocks, and deficit of acoustic power inside sunspots relative to surroundings.
  - Hard to use helioseismology to constrain sunspot subsurface structure. However, helioseismology has reveal interesting subsurface flows prior to emergence (Birch et al. 2019; Gottschling et al. 2021).

Homework

- Possible mini-projects:
  - Examine force (in)balance in different regions of a sunspot.
  - Produce cross-sectional plot of penumbral filament structure (check schematic diagram of Rempel 2009, ApJ).
  - Examine sunspot flux error as a function of optical depth, perhaps find a way to calibrate away this error.
  - Synthesize Stokes IQUV using the simulation data.
    - Degrade (blur + noise) for a given telescope point spread function.
- Read Rempel & Schlichenmaier (2011, Living Reviews)